Single-Cell Gene Expression Analyses Reveal Heterogeneous Responsiveness of Fetal Innate Lymphoid Progenitors to Notch Signaling.

Sylvestre Chea, Sandrine Schmutz, Claire Berthault, Thibaut Perchet, Maxime Petit, Odile Burlen-Defranoux, Ananda W Goldrath, Hans-Reimer Rodewald, Ana Cumano, Rachel Golub

Article

Cell Reports

Single-Cell Gene Expression Analyses Reveal Heterogeneous Responsiveness of Fetal Innate Lymphoid Progenitors to Notch Signaling

Graphical Abstract

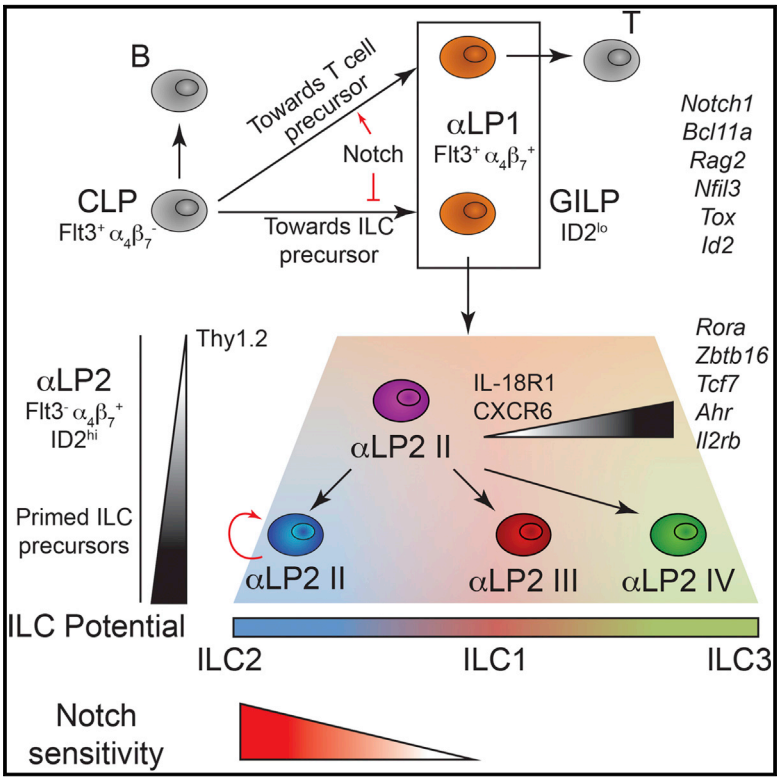

Highlights

- Global ILC progenitor and T precursors are found in the αLP1 compartment
- αLP2 compartment is heterogeneously composed of primed ILC precursors
- Notch signaling specifically acts on proliferation of an αLP2 ILC2 primed subset
- Constitutive NICD expression drives T cell development and restrains *Id2* expression

Authors

Sylvestre Chea, Sandrine Schmutz, Claire Berthault, ..., Hans-Reimer Rodewald, Ana Cumano, Rachel Golub

Correspondence

rachel.golub@pasteur.fr

In Brief

Molecular pathways and transcription factors involved in innate lymphoid cell (ILC) development are currently under intense investigation. Chea et al. now characterize different stages of ILC progenitors, from a global ILC progenitor (GILP) to committed ILC precursors, that are differentially sensitive to Notch signaling.

Chea et al., 2016, Cell Reports *14*, 1500–1516
February 16, 2016
http://dx.doi.org/10.1016/j.celrep.2016.01.015

OPEN ACCESS
CellPress

Cell Reports
Article

Single-Cell Gene Expression Analyses Reveal Heterogeneous Responsiveness of Fetal Innate Lymphoid Progenitors to Notch Signaling

Sylvestre Chea,[1,2,3] Sandrine Schmutz,[1,4] Claire Berthault,[1,2,3] Thibaut Perchet,[1,2,3] Maxime Petit,[1,2,3] Odile Burlen-Defranoux,[1,2,3] Ananda W. Goldrath,[5] Hans-Reimer Rodewald,[6] Ana Cumano,[1,2,3] and Rachel Golub[1,2,3,*]
[1]Lymphopoiesis Unit, Immunology Department, Institut Pasteur, 75015 Paris, France
[2]University Paris Diderot, Sorbonne Paris Cité, Cellule Pasteur, 75013 Paris, France
[3]INSERM U1223, 75015 Paris, France
[4]Cytometry Platform, Institut Pasteur, 75015 Paris, France
[5]Molecular Biology Section, Division of Biological Sciences, University of California, San Diego, La Jolla, CA 92093, USA
[6]Division of Cellular Immunology, German Cancer Research Center, 69120 Heidelberg, Germany
*Correspondence: rachel.golub@pasteur.fr
http://dx.doi.org/10.1016/j.celrep.2016.01.015

SUMMARY

T and innate lymphoid cells (ILCs) share some aspects of their developmental programs. However, although Notch signaling is strictly required for T cell development, it is dispensable for fetal ILC development. Constitutive activation of Notch signaling, at the common lymphoid progenitor stage, drives T cell development and abrogates ILC development by preventing *Id2* expression. By combining single-cell transcriptomics and clonal culture strategies, we characterize two heterogeneous $\alpha_4\beta_7$-expressing lymphoid progenitor compartments. αLP1 (Flt3$^+$) still retains T cell potential and comprises the global ILC progenitor, while αLP2 (Flt3$^-$) consists of ILC precursors that are primed toward the different ILC lineages. Only a subset of αLP2 precursors is sensitive to Notch signaling required for their proliferation. Our study identifies, in a refined manner, the diversity of transitional stages of ILC development, their transcriptional signatures, and their differential dependence on Notch signaling.

INTRODUCTION

Innate lymphoid cells (ILCs) are a family of three groups (ILC1, ILC2, and ILC3) that rapidly respond to inflammatory signals by producing cytokines also involved in tissue homeostasis (Seillet et al., 2014). Group 1 is defined as distinct from conventional NK (cNK) cells and requires T-bet for its lineage specification (Bernink et al., 2013; Daussy et al., 2014; Fuchs et al., 2013; Klose et al., 2014). Group 2 expresses the transcription factors GATA3 and RORα (Hoyler et al., 2012; Klein Wolterink et al., 2013; Wong et al., 2012). Group 3 developmentally depends on the transcription factor RORγt and is composed of several distinct populations that emerge during ontogeny. During fetal life, only lymphoid tissue inducer (LTi) cells are present, and other ILC3 subsets appear after birth. LTi cells and their precursors are found in the fetal liver (FL) (Mebius et al., 2001). They are essential for the generation of secondary lymphoid tissues (Eberl et al., 2004) and express *Rorc*, which controls interleukin (IL)-17A and IL-22 production. LTi cells are CCR6$^+$c-Kit$^+$IL-7Ra^{hi} cells and are referred to as LTi_4 and LTi_0, depending on the expression of CD4 (Klose et al., 2013; Sawa et al., 2010). All ILCs initially derive from the common lymphoid progenitor (CLP) (Cherrier et al., 2012; Mebius et al., 2001; Possot et al., 2011; Wong et al., 2012; Yang et al., 2011b). A common feature to ILC commitment is the requirement for the transcriptional repressor regulator ID2 (Hoyler et al., 2012; Moro et al., 2010; Satoh-Takayama et al., 2010; Yokota et al., 1999), an inhibitor of E protein transcription factors. The current scheme of ILC development describes the global ILC (GILP) precursor as NFIL3$^+$TOX$^+$, which further becomes the ID2^{hi} common helper ILC precursor (CHILP) when cNK cell potential is lost (Constantinides et al., 2014; Klose et al., 2014; Seehus et al., 2015; Xu et al., 2015). After acquisition of *Zbtb16* expression, CHILP loses the capacity to differentiate into LTi cells, showing that LTi precursors stand at the bifurcation between GILP and CHILP (Constantinides et al., 2014).

The Notch pathway is conserved and involved in many biological processes (Hori et al., 2013). Activation of Notch receptors promotes their proteolysis, resulting in the release of the Notch intracellular domain (NICD), which enters the nucleus as a co-transcriptional factor with the DNA-binding protein RBP-Jκ (Recombination signal sequence-Binding Protein Jκ chain) (Hori et al., 2013). The activation of this canonical Notch signaling pathway is known to regulate the transcription of target genes (Iso et al., 2003). During hematopoiesis, the Notch pathway acts as a cell-fate switch between the lymphoid and myeloid lineages (Oh et al., 2013). Notch1 is essential for T cell development at the expense of B cell development (Han et al., 2002; Pui et al., 1999; Sambandam et al., 2005). Notch2 signaling is crucial to marginal zone B cells (Saito et al., 2003; Tanigaki et al., 2002) and to the development of CD11b$^+$ classical dendritic cells (cDCs) in spleen and intestine (Lewis et al., 2011; Satpathy et al., 2013).

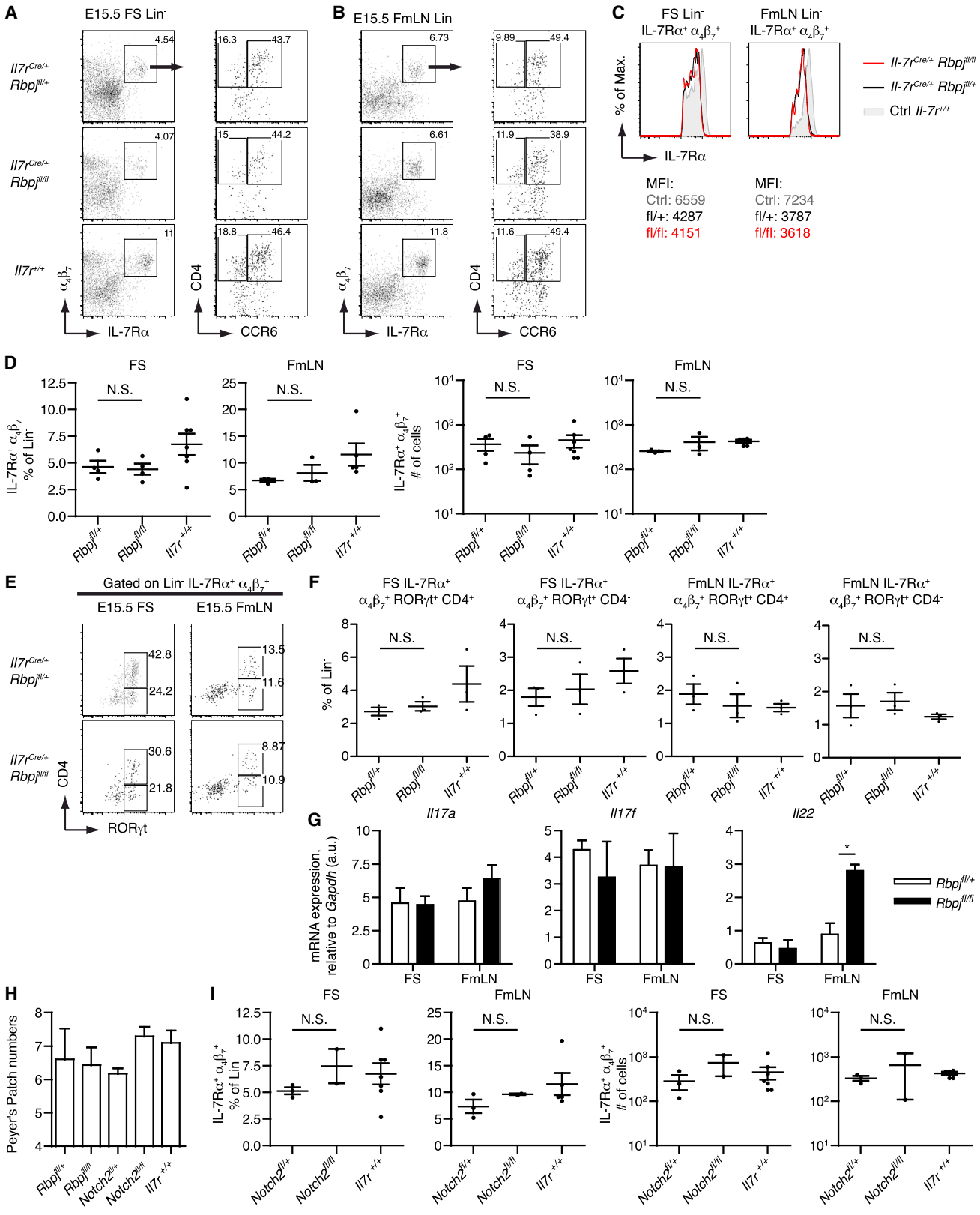

(legend on next page)

The relevance of the Notch pathway along ILC differentiation is still unresolved. Studies have supported the idea that the Notch pathway is necessary at a different branch point of adult ILC differentiation (Klose et al., 2013; Lee et al., 2012; Rankin et al., 2013). We recently suggested that Notch, although active, is not essential to the development of FL LTi cells (Possot et al., 2011), which was challenged by a report indicating that the Notch pathway blocks LTi development just before the expression of RORγt (Cherrier et al., 2012). Because both studies were performed in vitro, we developed mouse models to decipher the in vivo involvement of the Notch pathway during fetal LTi cell commitment and differentiation.

To delete the Notch pathway from the earliest stage of lymphoid progenitors, we used the *Il7r*^{Cre} mouse (Schlenner et al., 2010) combined with other mouse strains to either inactivate (*Rbpj*$^{fl/fl}$ and *Notch2*$^{fl/fl}$) or activate (*Rosa26*$^{loxP\text{-}Stop\text{-}loxP\text{-}NICD}$) Notch signaling. IL-7R is essential to drive lymphopoiesis and marks all lymphoid progenitors, as well as all ILCs, but not NK cells. IL-7 signaling provides the maintenance of lymphoid progenitors (Kondo et al., 1997) and is important for ILC development (Satoh-Takayama et al., 2010; Schmutz et al., 2009; Yoshida et al., 2002). Notch2 was previously shown to be more highly expressed in ILC precursors than Notch1 (Possot et al., 2011; Cherrier et al., 2012). In these mouse models, all the lymphoid progenitors and their progeny undergo Notch loss (or gain) of function. In parallel, we generated a double reporter *Id2*$^{yfp/+}$ *Cxcr6*$^{gfp/+}$ mouse to define diverse FL ID2$^+$ fractions of ILC precursors depending on the repartition of $\alpha_4\beta_7$, CXCR6, IL-18R1, and Thy1.2. We determined their hierarchy during ILC development and examined their equivalent in Notch-deficient embryos.

By targeting RBP-Jκ in lymphoid precursors, we report that canonical Notch signaling is unnecessary for LTi cell commitment and differentiation, and we showed that sustained Notch signaling is not blocking their development but rather promoting T cell development over any other lineages. In the periphery, Notch signaling modulates IL-22 levels in fetal mesenteric lymph node (FmLN) LTi cells. Finally, single-cell analysis of the expression of 81 mRNA transcripts revealed a hierarchy of differentiation, with heterogeneous fractions of lymphoid progenitors differentially enriched in ILC precursors. We demonstrate that Notch is only active on a sub-fraction mostly devoid of LTi fate. Notch signaling disruption changes the distribution of the ILC precursors and decreases the enrichment in *Hes1*$^+$/*Nfil3*$^+$ ILC precursors by regulating their proliferation. In conclusion, our study reveals the inherent cellular and developmental, context-dependent nature of canonical Notch signaling during fetal ILC commitment and differentiation.

RESULTS

Inactivation of the Notch Signaling Pathway Does Not Affect the Capacity of LTi Cells to Colonize the Lymph Node Anlagen but Alters Their Cytokine Production

We evaluated the in vivo role of Notch in the development of LTi cells in *Il7r*$^{cre/+}$*Rbpj*$^{fl/fl}$ and *Il7r*$^{Cre/+}$*Rbpj*$^{fl/+}$ embryos, where Notch signaling is inactivated in all lymphoid cells. All Lin$^-$ IL-7Rα$^+$ cells were yellow fluorescent protein positive (YFP$^+$), indicating that recombination efficiently occurred in all FL lymphoid precursors (Figure S1A). We also ascertain deletion of *Rbpj* using genomic PCR and detected less than 1% of failed *Rbpj* deletion (Figure S1B). A complete block at the DN1 (CD44$^+$CD25$^-$) stage was observed in the thymus of embryonic day (E)15.5 *Il7r*$^{Cre/+}$ *Rbpj*$^{fl/fl}$ but not in *Rbpj*$^{fl/+}$ embryos (Figure S1C). We analyzed lymphoid subsets of E15.5 fetal spleen (FS) and FmLNs in *Rbpj*-deleted embryos. $\alpha_4\beta_7^+$ progenitors (αLP) and LTi cells, as well as subfractions LTi_0 and LTi_4, were present in similar proportion and numbers after Notch inactivation (Figures 1A–1F). In all *Il7r*$^{Cre/+}$ embryos, the mean fluorescence intensity (MFI) for the IL7Rα was lower than in control *Il7r*$^{+/+}$ embryos (Figure 1C). We quantified their levels of *Il17a*, *Il17f*, and *Il22* transcripts. While *Il17a* and *Il17f* levels were identical, *Il22* mRNA levels were significantly higher in lymph node LTi cells after *Rbpj* deletion (Figure 1G). Moreover, in Notch-deficient mice, Peyer's patches formed in normal numbers (Figure 1H), and all types of peripheral lymph nodes were present, indicating that LTi cells' function as inducer cells is independent of Notch activation.

In peripheral LTi cells (FS and FmLN), *Notch2* is expressed in higher amounts than *Notch1* (Figure S1D). The inactivation of Notch signaling significantly interferes with the *Notch2* levels in lymphoid cells from the FmLNs (Figure S1D). No differences were observed for the frequency and total numbers of peripheral lymphoid progenitors from *Il7r*$^{cre/+}$*Notch2*$^{fl/fl}$ and *Il7r*$^{cre/+}$ *Notch2*$^{fl/+}$ embryos (Figure 1I). The distribution and phenotype of RORγt$^+$ LTi in both FS and FmLNs were also similar, indicating that these progenitors develop and migrate independently of Notch2 (Figures S1E and 1F).

In conclusion, although not required for the development, migration, and the functional property of secondary tissue

Figure 1. Notch Signaling Disruption Does Not Affect Peripheral Colonization of LTi Cells or LTi Function but Alters Cytokine Production

(A and B) Flow cytometry of FS (A) and FmLNs (B) for the presence of Lin$^-$ (Lin: CD3, CD11c, CD19, Ter119, Gr1, NK1.1) IL-7Rα$^+$, α4β7$^+$, and CD4 and CCR6 expression in those cells in Il7r$^{Cre/+}$ Rosa26YFP Rbpj$^{fl/+}$, Rbpj$^{fl/fl}$, or Il7r$^{+/+}$ embryos at E15.5.

(C and D) IL-7Rα MFI (C), percentages, and absolute numbers (D) of the different fractions analyzed in (A) and (B).

(E) Flow cytometry of E15.5 FS and FmLN Lin$^-$ IL-7Rα$^+$ $\alpha_4\beta_7^+$ cells for CD4 and RORγt expression.

(F) Percentages of IL-7Rα$^+$ $\alpha_4\beta_7^+$ RORγt$^+$ CD4$^+$ or CD4$^-$ cells of Lin$^-$ in FS or FmLN from *Il7r*$^{Cre/+}$ *Rosa26*^{YFP} *Rbpj*$^{fl/+}$, *Rbpj*$^{fl/fl}$, or *Il7r*$^{+/+}$ embryos at E15.5.

(G) RT qPCR analysis of *Il17a*, *Il17f*, and *Il22* in sorted Lin$^-$ IL-7Rα$^+$ $\alpha_4\beta_7^+$ cells from *Il7r*$^{Cre/+}$ *Rosa26*^{YFP}, *Rbpj*$^{fl/+}$, or *Rbpj*$^{fl/fl}$ E15.5 FS and FmLN after 3 hr of PMA (phorbol 12-myristate 13-acetate)/ionomycin activation. Results are presented relative to *Gapdh* (a.u.).

(H) Peyer's patch counts in adult Il7r$^{Cre/+}$ Rosa26^{YFP} Rbpj$^{fl/+}$, Rbpj$^{fl/fl}$, Notch2$^{fl/+}$, Notch2$^{fl/fl}$, and control Il7r$^{+/+}$ mice.

(I) Percentages and absolute numbers of E15.5 FS and FmLN Lin$^-$ IL-7Rα$^+$ $\alpha_4\beta_7^-$ CD4$^+$ *Il7r*$^{Cre/+}$ *Rosa26*^{YFP} *Notch2*$^{fl/+}$, *Notch2*$^{fl/fl}$, or control *Il7r*$^{+/+}$ mice.

Data are representative of at least three independent experiments (A, B, C, and E) ($n \geq 4$), three pooled independent experiments (D, F, and I) ($n = 3$), three independent experiments (G), or at least five pooled independent experiments (H) ($n \geq 5$). In (D), (F), and (I), each dot represents a single experiment. Statistical data show mean ± SEM. *$p < 0.05$ (unpaired Student's t test). N.S., not significant.

See also Figure S1.

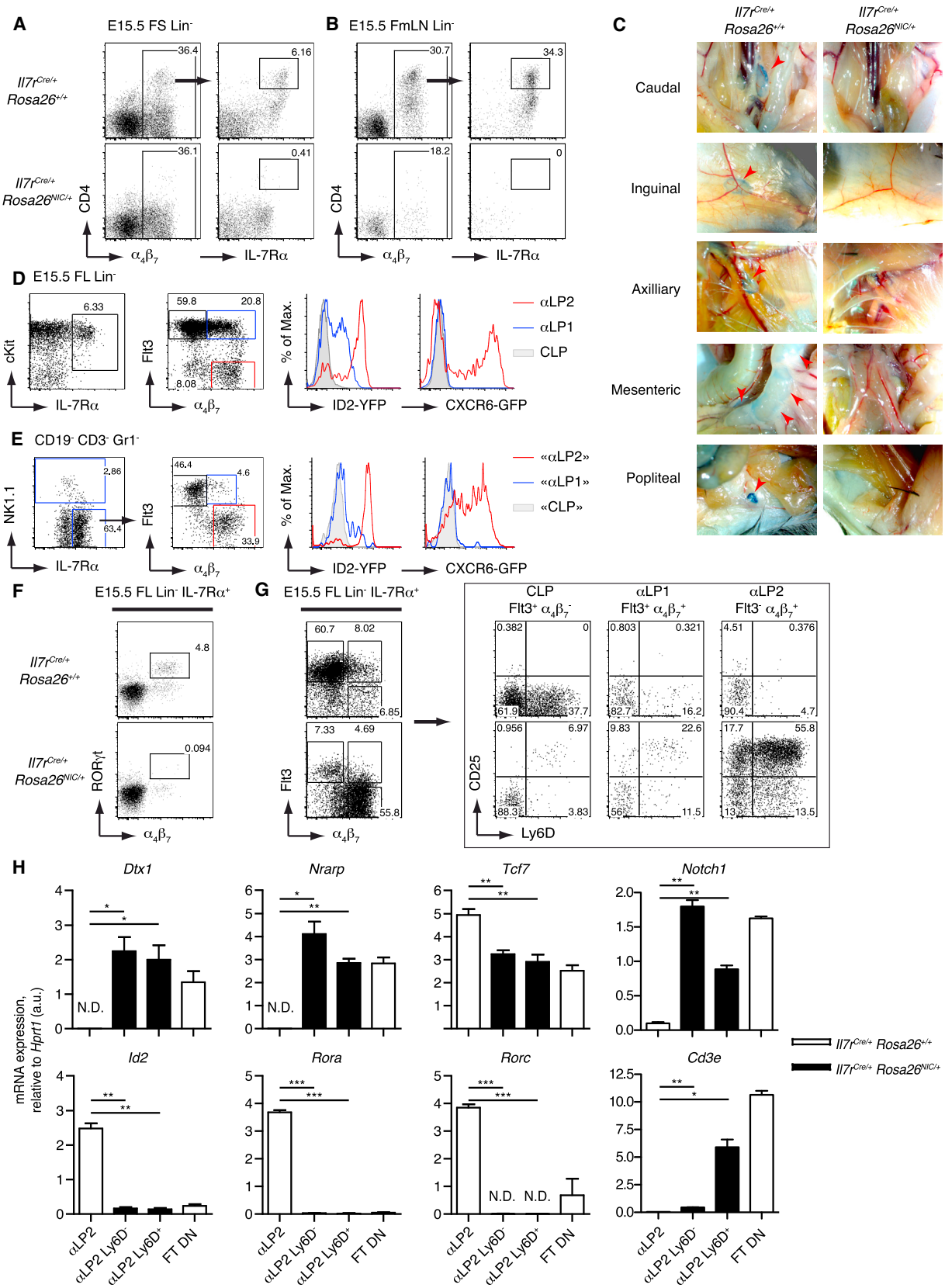

(legend on next page)

inducer, Notch activity only determines the profile of cytokine secretion of LTi cells in the periphery.

Constitutive Expression of the NICD Forces Lymphoid Precursors into T Cell Differentiation

Since Notch signaling is dispensable for the migration and function of LTi cells as secondary lymphoid organ inducers, we questioned whether persistent Notch signaling could modulate their functions and/or differentiation; therefore, we generated *Il7r*$^{Cre/+}$*Rosa26*^{NIC}, where Notch is constitutively active in lymphoid cells. In peripheral FS and FmLNs, RORγt$^+$ cells were undetectable (Figures 2A and 2B), and no lymph node were found in adult *Il7r*$^{Cre/+}$*Rosa26*^{NIC} mice (Figure 2C).

Analysis of the E15.5 *Id2*$^{yfp/+}$*Cxcr6*$^{gfp/+}$ FL compartment shows that CLPs (Flt3$^+\alpha_4\beta_7{}^-$) do not express YFP or GFP, whereas αLP, either Flt3$^+$ (named αLP1) or Flt3$^-$ (named αLP2), express different levels of ID2 (Figure 2D). αLP1 expressed intermediate levels of ID2, suggesting that the upregulation of ID2 begins within this subset. After short-term cultures, CLPs are able to give rise to both αLP1 and αLP2 fractions (Figure 2E). ID2 expression is detected in few αLP1 cells and in most αLP2 cells. Also, αLP2 expressed high levels of YFP contrary to the αLP1 fraction. In conclusion, αLP1 is a transitional stage between CLP and αLP2 with few ID2^{lo} progenitors. ID2^{hi} cells are highly represented in αLP2 (84.6%).

In embryos with constitutive Notch signaling activation, no $\alpha_4\beta_7{}^+$RORγt$^+$ cells could be detected in the FL (Figure 2F). Cells harboring a CLP phenotype were decreased, whereas those presenting an αLP2 phenotype were increased (Figure 2G). However, the αLP2 subset in *Il7r*$^{Cre/+}$*Rosa26*^{NIC} FL now comprises a majority of CD25$^+$Ly6D$^+$ cells not present in the control (Figure 2G), but resembling DN2-DN3 CD25$^+$Ly6D$^+$ from normal E15.5 thymocytes (data not shown). To determine whether the *Il7r*$^{Cre/+}$*Rosa26*^{NIC} αLP2 cells are composed of ID2$^+$ ILC progenitors or T cell progenitors, we quantified the expression of transcripts mutually exclusive to T cell progenitors (*Cd3e*, *Notch1*, *Dtx1*, *Nrarp*) or ILC progenitors (*Id2*, *Rora*, and *Rorc*) (Figure 2H). *Tcf7* is a possible target of the Notch pathway and is expressed by both T and ILC progenitors. The FL αLP2 fraction expressed undetectable levels of T cell-related gene mRNA in controls. However, both Ly6D$^-$ and Ly6D$^+$ αLP2 from *Il7r*$^{Cre/+}$*Rosa26*^{NIC} FL expressed these T cell progenitor transcripts but failed to express ILC transcripts (Figure 2H). We concluded that the constitutive activation of the Notch pathway committed all CLPs toward the T cell pathway.

Inactivation of the Notch Signaling Pathway Does Not Alter the Phenotype, Distribution, or Differentiation Capacities of FL Lymphoid Progenitors

We analyzed the development of lymphoid progenitors in FL from embryos with an inactive or functional canonical Notch pathway. In all embryos, lymphoid progenitors displayed a similar pattern of c-Kit, Sca1, Flt3, and $\alpha_4\beta_7$ expression (Figure 3A). The IL7Ra levels were similarly lower in all FL compartments that have only one IL7Ra allele (*Il7r*$^{Cre/+}$), compared to wild-type (WT) control (Figure 3B). However, concerning the αLP2 subset, the distribution of IL7Rα^{hi} cells may be different after notch disruption (Figure 3B). Numbers of lymphoid progenitors were consistently lower in mice with only one allele of the IL-7Rα (*Il7r*$^{Cre/+}$), although the percentages of Lin$^-$IL-7Rα$^+$ cells are similar and the representation of the different subsets within IL-7Rα$^+$ cells is unchanged. RORγt$^+$ cells represented a comparable subset of αLP2 in all genotypes (Figure 3A), and no statistical difference was detected in percentages and numbers of CLP, αLP1, αLP2, and LTip isolated from *Il7r*$^{Cre/+}$*Rbpj*$^{fl/fl}$ or littermate controls (*Il7r*$^{Cre/+}$*Rbpj*$^{fl/+}$) (Figure 3C).

We sorted the different precursor subsets (Figure S2A) and show that the level of *Notch1* transcripts decreases as differentiation into ILCs progresses from the CLP stage to the αLP2 stage, whereas *Notch2* transcripts reach maximal levels in αLP2 cells (Figure S2B). Because *Notch2*, but not *Notch1*, is highly expressed in ILC progenitors, and as non-canonical Notch signaling might operate in the absence of RBP-Jκ, we analyzed ILC development after *Notch2* deletion in lymphoid progenitors. Neither the phenotype, percentage, and numbers of FL lymphoid precursors (Figures S2C and S2D) nor T cell development (Figure S2E) were affected by the *Notch2* deletion.

Short-term cultures were performed to analyze the capacity of lymphoid progenitors to upregulate $\alpha_4\beta_7$ in the absence or presence of Notch signaling (Figure 3D). After 48 hr on OP9 stroma, around 35% of cultured CLPs expressed $\alpha_4\beta_7$ regardless of the genotypes. Upregulation of $\alpha_4\beta_7$ was also observed on OP9-DL4 for all genotypes (Figure 3E). Consistent with Notch deficiency, we observed the development of CD19$^+$ B cells on

Figure 2. Overexpression of the Notch Pathway Is Not Blocking the ILC Precursors at an Early Stage but Rather Instructs Strong T Cell Differentiation from Earliest Stages of the CLP

(A and B) Flow cytometry of E15.5 FS (A) and FmLN (B) for the presence of Lin$^-$IL-7Rα$^+\alpha_4\beta_7{}^+$CD4$^+$ cells in E15.5 *Il7r*$^{Cre/+}$*Rosa26*$^{+/+}$ or *Il7r*$^{Cre/+}$ *Rosa26*$^{NIC/+}$ embryos.

(C) Pictures of lymph nodes in adult *Il7r*$^{Cre/+}$*Rosa26*$^{+/+}$ or *Il7r*$^{Cre/+}$*Rosa26*$^{NIC/+}$ mice (6 to 10 weeks old), injected with China ink 2 hr prior to analysis.

(D) Flow cytometry of FL cells from *Id2*$^{YFP/+}$*Cxcr6*$^{GFP/+}$ E15.5 embryos. Lin$^-$IL-7Rα$^+$ is fractionated according to Flt3 and $\alpha_4\beta_7$ expression, and expression of ID2-YFP or CXCR6-GFP is assessed in CLP (filled gray, Flt3$^+\alpha_4\beta_7{}^-$), αLP1 (blue, Flt3$^+\alpha_4\beta_7{}^+$), and αLP2 (red, Flt3$^-\alpha_4\beta_7{}^+$) compartments.

(E) Short-term culture of 10,000 CLPs from E15.5 *Cxcr6*$^{GFP/+}$*Id2*$^{YFP/+}$ FL on OP9 cells for 3 days, with IL-7, cKitL, and Flt3L. Histogram shows ID2-YFP and CXCR6-GFP expression levels from in-vitro-generated CLP (filled gray), αLP1 (blue), or αLP2 (red) cells.

(F) Flow cytometry of E15.5 FL cells from *Il7r*$^{Cre/+}$*Rosa26*$^{+/+}$ or *Rosa26*$^{NIC/+}$ for LTip (Lin$^-$IL-7Rα$^+$RORγt$^+\alpha_4\beta_7{}^+$).

(G) Flow cytometry of E15.5 FL cells from *Il7r*$^{Cre/+}$*Rosa26*$^{+/+}$ or *Rosa26*$^{NIC/+}$. Each compartment, as defined in (D), is respectively analyzed for CD25 and Ly6D expression.

(H) RT qPCR analysis of various transcripts in αLP2 Ly6D$^-$ or αLP2 Ly6D$^+$ in *Il7r*$^{Cre/+}$*Rosa26*$^{NIC/+}$ (black) or αLP2 in *Il7r*$^{Cre/+}$*Rosa26*$^{+/+}$ (white) E15.5 FL, presented relative to *Hprt* (a.u.). Cells from *Il7r*$^{Cre/+}$*Rosa26*$^{+/+}$ E15.5 fetal thymus (FT DN) sorted as CD3$^-$CD4$^-$CD8$^-$CD44$^{hi}\alpha_4\beta_7{}^+$ were used as controls.

Data are representative of at least three independent experiments—(F), (G), and (H) from single FL each and (A), (B), and (D) from pooled organs—or three independent experiments (C) ($n \geq 3$ for each group), or three independent experiments with at least two wells per experiment (E). Statistical data show mean ± SEM. *$p < 0.05$; **$p < 0.01$; ***$p < 0.001$ (unpaired Student's t test). N.D., not detected.

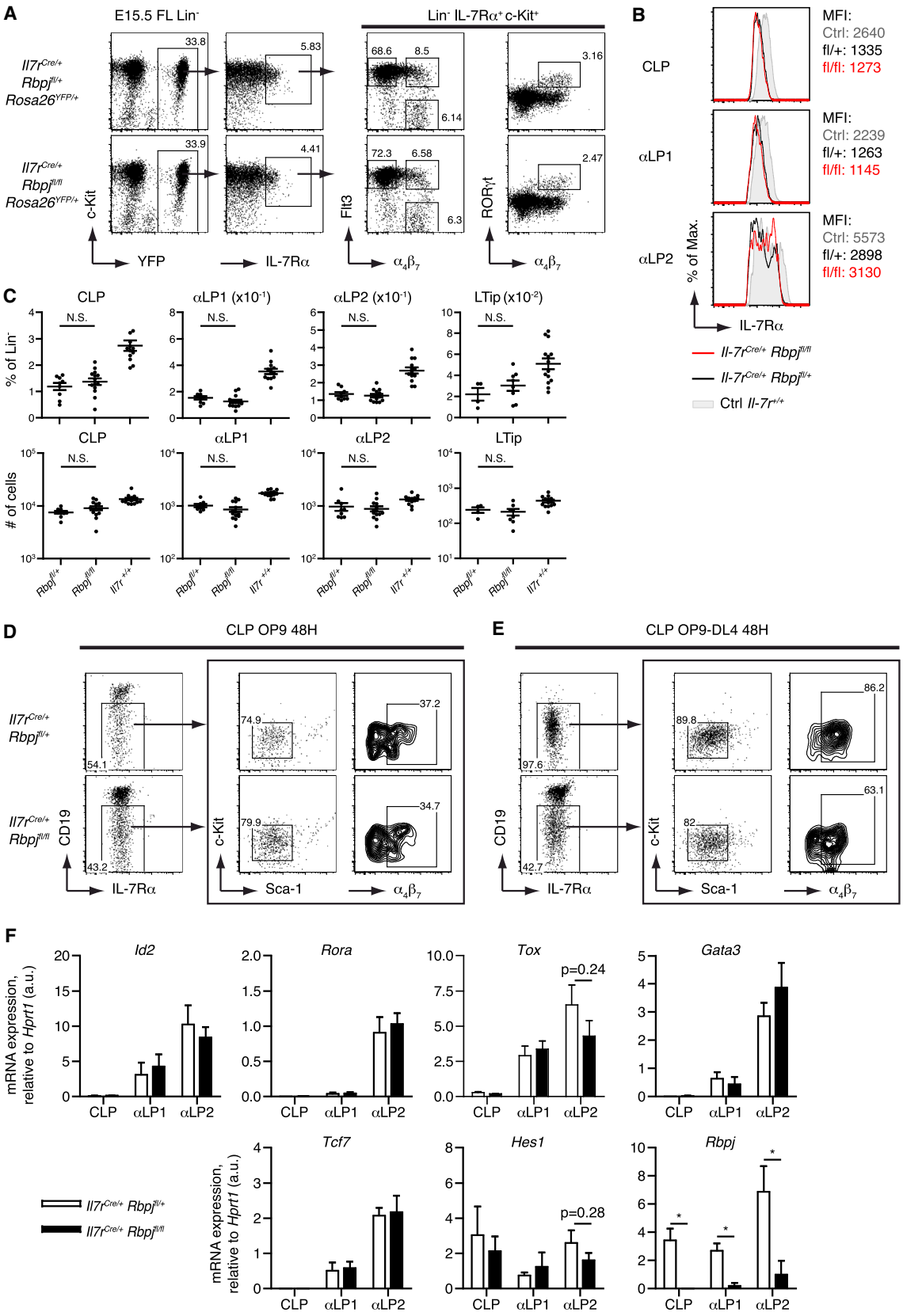

(legend on next page)

OP9-DL4 from CLPs isolated from *Il7r*$^{Cre/+}$*Rbpj*$^{fl/fl}$ embryos (Figure 3E). However, fewer progenitors have progressed to the $\alpha_4\beta_7^+$ stage in Notch-defective embryos.

The differentiation potential of αLP1 and αLP2 from Notch-deficient or Notch-competent embryos was tested after 8 days of culture. As expected, T cell differentiation potential was lost in Notch-deficient αLP1 cells, but not in their littermate controls, and the NK cell progeny increased proportionally to the loss of *Rbpj* alleles (Figure S2F). In αLP1 cells from *Il7r*$^{Cre/+}$*Rbpj*$^{fl/fl}$, $\alpha_4\beta_7$ expression was sustained, and similar proportions of RORγt$^+$ cells were obtained (Figures S2F and S2G). Because the αLP2 fraction already contains RORγt$^+$ cells, only the detection of NK cells was considered as differentiation.

Fetal lymphoid precursors and peripheral LTi cells express Notch receptors, and the ligand Delta1 was found in FL (Cherrier et al., 2012), suggesting a probable Notch activation of these cells. However, the Notch pathway abrogation did not impact on FL lymphoid progenitor numbers or phenotype. Hence, we examined whether Notch was activated by quantifying the mRNA expression of its key target genes (*Tcf7*, *Hes1*, *Gata3*, *Dtx1*, and *Nrarp*) and ILC transcripts (*Id2*, *Rora*, *Tox*) in E15.5 FL of *Il7r*$^{Cre/+}$*Rbpj*$^{fl/+}$ and *Rbpj*$^{fl/fl}$ embryos (Figure 3F). *Dtx1* and *Nrarp* were not expressed (data not shown). Except for *Rora* (only found in αLP2) and *Hes1* (also expressed in CLPs), the expression of most transcription factors analyzed begins at the αLP1 stage (Figure 3F). No statistical difference was detected in the expression levels of *Id2*, *Tcf7*, *Gata3* and *Rora* after the inactivation of the Notch pathway. We noticed a tendency for *Hes1* and *Tox* mRNA levels to decrease after disruption of the Notch pathway (Figure 3F).

In conclusion, the inactivation of the Notch pathway did not alter the capacity of FL lymphoid precursors to differentiate into ILCs. The Notch signaling pathway appears to be dispensable to generate and maintain the phenotype and distribution of FL lymphoid progenitors, including RORγt$^+$ LTip. However, it is probably implicated during the differentiation of specific ILC subsets, since some ILC-specific transcription factors tend to be decreased after Notch disruption. Hence, frequency and heterogeneity of αLP2 subsets may vary after disruption of the Notch pathway.

αLP2 Cells Have Heterogeneous Transcriptional Profiles at the Single-Cell Level

The heterogeneity of ILC progenitors drove us to develop a single-cell transcriptional analysis assay using the Biomark HD system to assess the effect of Notch signaling. The linearity, specificity, and efficiency of primers have been thoroughly tested (Figures S3A–S3E; Tables S1 and S2). We sorted single αLP1 and αLP2 cells from both Notch-competent and -deficient FL and analyzed the expression of 81 genes. Among the sorted single cells, only cells that expressed the three housekeeping genes (*Actb, Gapdh*, and *Hprt*) and more than 10% of the 81 selected genes were considered (Figure S4A). Analysis of single-cell transcriptional expression allowed the identification of common signatures and key gene signatures that distinguish αLP1 from αLP2 cells. αLP1 and αLP2 share expression of ILC transcription factors such as *Tox*, *Ets1*, *Id2*, and *Nfil3* and the absence of expression of specific B cell genes (*Pax5* or *Ebf1*) (Figure S4B). αLP1 cells are enriched in cells expressing *Notch1*, *Rag2*, and *Bcl11a*, which are characteristics of T cell progenitors. On the other hand, αLP2 cells mostly express *Zbtb16*, *Rora*, *Tcf7*, and *Il2rb* but have no expression of *Rag2* and *Bcl11a* (Figure S4C).

We have focused on the αLP2 subset analysis to avoid any T cell progenitor contaminant. After hierarchical clustering, we could define four clusters, based on the expression pattern of 43 discriminative genes regardless of the Notch deficiency. Using the Notch-competent condition as a control, we identified four groups of genes that could define specific transcriptional signatures (Figure 4A).

All clusters shared a core αLP2 gene signature composed of the expression of *Itga4*, *Ets1*, *Notch2*, *Rora*, *Foxo1*, *Hif1a*, *Nfatc1*, and *Zbtb16* (Figure 4B). Cluster I (αLP2 I) is substantially different from other clusters, as it has a halved *Id2*-expressing cell frequency, with lower expression levels of *Id2* by the few expressing cells (Figure S4D) and neither *Tox* nor *Tcf7* expression, which are key transcription factors required for ILC development. In contrast, almost all cells in clusters II, III, and IV expressed those genes, along with *Ahr, Il2rb*, and *Tnfrsf1a*. Furthermore, cluster I displays a unique gene signature distinct from that of ILCs (Figure 4C).

Further discrimination of cluster II from clusters III and IV is based on the expression of *Cxcr6* and *Il18r1* (Figure 4D). Key molecules for LTi cell function, such as *Lta*, *Ltb*, and *Cxcr5*, are also highly enriched in clusters III and IV. In contrast, cluster II is mostly characterized by the expression of transcription factors *Gata3*, *Nfil3*, and *Bcl11b*, suggesting enrichment in the ILC2 progenitor transcriptional profile. Interestingly, *Hes1*, a target of Notch signaling, was found at high frequency in cluster II, suggesting a possible Notch activity in this subset.

Finally, cluster III is enriched in cells expressing key NK genes such as transcription factors *Tbx21*, *Eomes*, *Irf1*, and *Irf8*, whereas cells expressing *Rorc*, *Bcl2*, and *Il1r1*, key features of LTi or LTip cells, constitute cluster IV (Figure 4E).

Figure 3. ILC3 FL Progenitors Are Maintained after In Vivo Disruption of the Notch Pathway

(A) Flow cytometry of E15.5 FL cells from *Il7r*$^{Cre/+}$ *Rosa26*^{YFP}, *Rbpj*$^{fl/+}$, or *Rbpj*$^{fl/fl}$ mice for the presence of CLP, αLP1, αLP2, and LTip cells.

(B and C) IL-7Rα MFI (B) and percentages and absolute numbers (C) of the different fractions analyzed in (A).

(D and E) Differentiation potential of E15.5 FL-derived CLP from *Il7r*$^{Cre/+}$ *Rosa26*^{YFP} *Rbpj*$^{fl/+}$ or *Rbpj*$^{fl/fl}$ mice cultured for 48 hr on OP9 (D) or OP9-DL4 (E) with Kit-L, Flt3-L, IL-2, and IL-7 (50 cells per well).

(F) RT qPCR analysis of various transcripts in CLP, αLP1, or αLP2 cells from *Il7r*$^{Cre/+}$ *Rosa26*^{YFP} *Rbpj*$^{fl/+}$ (white bars) or *Rbpj*$^{fl/fl}$ (black bars) E15.5 FL, presented relative to *Hprt* (a.u.).

Data are representative of at least four independent experiments (A–C; from single FL each, n ≥ 4), or at least six wells from two independent experiments (D and E), or from three pooled independent experiments (F). In (C), each dot represents a single FL. Statistical data show mean ± SEM. *p < 0.05 (unpaired Student's t test). Statistical data show mean ± SEM. *p < 0.05 (unpaired Student's t test). N.S., not significant.

See also Figure S2.

A

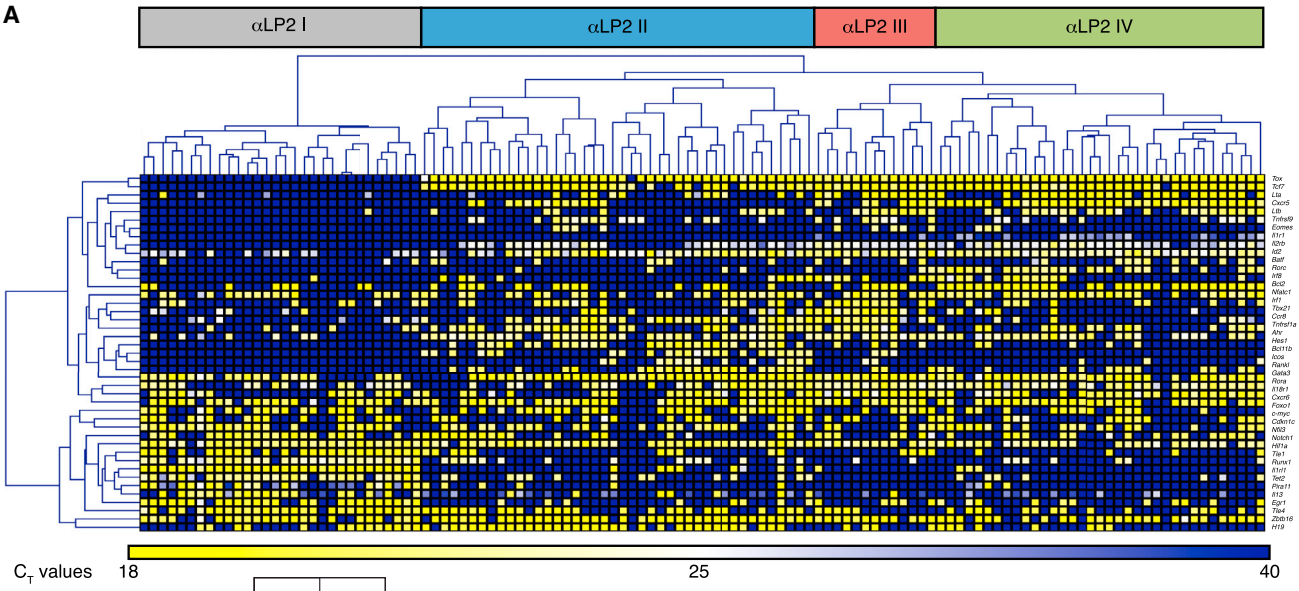

E15.5 FL Lin⁻ IL-7Rα⁺
Il7r$^{Cre/+}$ *Rbpj*$^{fl/+}$ or *Rbpj*$^{fl/fl}$

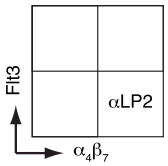

B Common αLP2 signature

	I	II	III	IV
Hif1a	100	93	100	79
Ets1	100	96	100	100
Foxo1	91	82	83	90
Notch2	91	93	100	100
Zbtb16	82	96	100	74
Rora	73	96	100	84
Itga4	73	96	100	100
Nfatc1	64	63	67	84
Bcl11a	0	3,7	0	0
Il23r	0	0	0	5,3
Cxcl2	0	7,4	0	5,3
Tnfrsf1b	0	0	0	0

C ILCp (II.III.IV) signature

	I	II	III	IV
Id2	46	93	100	100
Tox	0	100	100	100
Tcf7	0	82	100	100
Ahr	18	82	100	84
Il2rb	0	74	100	90
Tnfrsf1a	18	67	67	47
Batf	0	19	17	21
Pira11	64	11	0	16
Tle1	73	22	17	5.3
Egr1	73	22	17	26
Il13	73	44	17	42
Runx1	91	33	0	26
Tet2	91	33	0	21
Il1rl1	100	22	0	5.3
Notch1	91	37	50	42
Tle4	91	59	50	37

D ILC2p (II) vs III.IV signature

	I	II	III	IV
Il18r1	55	56	100	90
Cxcr6	27	52	100	79
Lta	9.1	33	83	68
Cxcr5	0	37	67	95
Ltb	0	22	50	63
Icos	0	26	33	5.3
Bcl11b	0	52	17	0
Gata3	0	56	33	32
Hes1	0	78	33	16
Ccr8	0	74	100	16
H19	27	93	67	11
c-myc	55	70	33	53
Nfil3	73	74	50	47

E NKp (III) vs LTip (IV) signature

	I	II	III	IV
Bcl2	36	41	50	84
Rorc	0	15	17	74
Il1r1	0	0	0	47
Eomes	0	7.4	50	11
Tnfrsf9	0	37	67	32
Cdkn1c	36	30	50	26
Irf8	9.1	15	83	42
Tbx21	18	22	83	16
Irf1	27	41	100	37

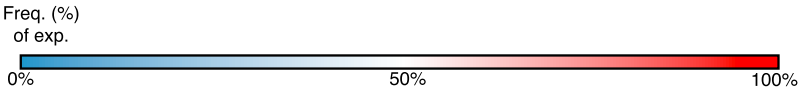

Figure 4. Single-Cell Transcriptional Analysis of FL αLP2

(A) RT qPCR analysis of single αLP2 from *Il7r*$^{Cre/+}$*Rbpj*$^{fl/+}$ or *Rbpj*$^{fl/fl}$ E15.5–E17.5 FL using the Biomark HD system. Each column represents a single cell, and each line represents a gene. Single cells are clustered, and four clusters are identified: αLP2 I (gray), αLP2 II (blue), αLP2 III (red), and αLP2 IV (green). Gradient represents the C_T value for each gene and each single cell (yellow = high expression, white = low expression, and dark blue = no expression; C_T > 40).

(legend continued on next page)

E15.5 FL lymphoid progenitors were tested for the presence of GATA3, T-bet, EOMES, and RORγt. Only GATA3$^+$ and RORγt$^+$ cells were detected in the αLP2 fraction (Figure S5A). Hence, the expression of both *Tbx21* and *Eomes* mRNA show that specific mature ILC genes already have an accessible chromatin at the precursor stage. GATA3 is known to be necessary for the development of ILC3 and then could be considered as an ILC progenitor transcription factor (Serafini et al., 2014). Clonal cultures on OP9 stromal cells of αLP2 RORγt$^+$ cells demonstrate that some RORγt-expressing cells could still be considered as ILC progenitors. Indeed, RORγt^{lo}IL-7Rα$^+$ cells retain the capacity to give rise to both NK (NK1.1$^+$) and ILC2 (ICOS^{hi}α$_4$β$_7^-$CD25$^+$RORγt$^-$) cells, contrary to RORγt^{hi}IL-7Rα$^+$ cells (Figures S5B–S5D). Moreover, frequencies of the progeny obtained from the clonal assay suggest that αLP2 RORγt^{lo} progenitors represent a heterogeneous compartment (Figure S5D). Hence, despite the expression of specific mature ILC transcripts, the FL αLP2 fraction is still heterogeneously composed of ILC progenitors.

In conclusion, we identified four subsets within the αLP2 fraction, each enriched in a specific ILC progenitor type. The clustering and the gene signatures suggest that the "αLP2 I" is enriched in *Id2*$^-$ cells, representing a population of non-T/B progenitors. The "αLP2 II" represents ILC precursors with an enrichment in ILC2 fate, whereas "αLP2 III" is mainly constituted of NK progenitor cells, and the "αLP2 IV" mainly consists of LTi progenitors.

Heterogeneity of αLP2 Cells Reveals Different Priming toward ILC Lineages

To discriminate αLP2 subsets as defined previously, Thy1.2 and IL-18R1 expression were analyzed jointly with CXCR6 and ID2 expression due to *Id2*$^{yfp/+}$ *Cxcr6*$^{gfp/+}$ embryos.

The heterogeneous levels of ID2 in the αLP2 compartment (Figure 2D) are in agreement with the single-cell assay showing diverse transcriptional levels of *Id2* gene expression (Figure 4C; Figure S4). All ID2$^-$ αLP2 cells are Thy1.2$^-$IL-18R1^{lo} (Figure 5A). ID2$^+$CXCR6$^-$ αLP2 cells are IL-18R1$^-$ and could be subdivided into Thy1.2$^-$ and Thy1.2$^+$. CXCR6$^+$ cells that are all ID2$^+$ also express IL-18R1 and Thy1.2 (Figure 5A). Hence, the combination of Thy1.2 and IL-18R1 enables the ex vivo subdivision of αLP2 subsets in embryos that are not tagged for ID2 or CXCR6 (Figure 5B). As observed in Figure 5C, the αLP2 II subset concerns Id2$^+$CXCR6$^-$ cells that could be isolated as IL-18R1$^-$ cells. The Id2$^+$CXCR6$^-$ subset is further separated into two main fractions depending on the expression of Thy1.2 (Figure 5B, Thy1.2$^+$IL-18R1$^-$ in blue and Thy1.2$^-$IL-18R1$^-$ in violet). Id2$^+$CXCR6$^+$ cells could be isolated as Thy1.2$^+$IL-18R1$^+$ cells and correspond to the αLP2 fractions III + IV. Finally, the Thy1.2$^-$IL-18R1$^+$ cells correspond to the αLP2 I cells.

We assessed the clonal in vitro potential of the CLP, αLP1, and αLP2 fractions (Figure 5C). After 8 days of culture on OP9-DL4, progeny cells were identified as either T progenitors (Lin$^-$ID2$^-$CD25$^+$) or ILCs (Lin$^-$ID2$^+$) that could be divided into NK1.1$^+$ ILC1, ICOS^{hi}α$_4$β$_7^-$ ILC2, or ICOS^{lo}α$_4$β$_7^{hi}$CXCR6^{hi} ILC3 (Figure 5D). αLP2 I barely gave rise to any cells in culture conditions promoting lymphoid development. CLP and αLP1 subsets have a clonal efficiency of 40%, whereas αLP2 II Thy1.2$^-$ or Thy1.2$^+$, III and IV have a clonal efficiency of 50% (Figure 5E). As suspected by the absence of Id2 gene expression and a specific gene signature, αLP2 I cells do not comprise ILC precursors.

CLPs mainly gave rise to T cells, with less than 5% of the progenitors that developed into ILCs alone. The αLP1 compartment retains T cell potential and could give rise to all ILC subsets, confirming our assumption from the transcriptome analysis that early ILC progenitors are represented in this fraction (Figure S3). All ILCs could be detected within single clones at very low frequencies (less than 7%, with or without T cells; Figure 5F). By using the sorting index, we observed that, among the αLP1 subset, ILC precursors are ID2^{med}α$_4$β$_7^{hi}$, whereas T progenitors are ID2$^-$α$_4$β$_7^+$ (data not shown). The αLP2 compartments, as previously reported, had no T cell potential (Possot et al., 2011). Interestingly, the subpopulations have distinctive ILC differentiation potentials (Figure 5G). No cell producing all ILC lineages could be detected at this frequency. Interestingly, each subpopulation preferentially gives rise to one ILC group. αLP2 II Thy1.2$^-$ cells mainly generate ILC1, as well as a fair proportion of ILC3. αLP2 II Thy1.2$^+$ cells preferentially give rise to ILC2. Finally, αLP2 III/IV cells are enriched in RORγt$^+$ cells and then are biased toward ILC3, but they may also differentiate into ILC1.

In conclusion, we report that the αLP1 compartment, which contains a frequent tripotent ILC lineage precursor, is upstream of the αLP2 compartment. This latter can be subdivided in three subsets according to the surface expression of IL-18R1 and Thy1.2, and these subsets are differentially primed for differentiation toward each ILC lineage.

Notch Deficiency Differentially Affects αLP2 Subsets

We included and compared the Notch-deficient cells to our single-cell analysis to assess the extent of Notch activity in these compartments. Principal-component analysis (PCA) shows that within each cluster, Notch-competent and Notch-deficient cells are overlapping, suggesting that the major key gene signatures could still be found in the absence of Notch (Figures 6A and 6B). We first studied the frequency of *Id2*$^+$ over *Id2*$^-$ progenitors in both genotypes and noticed that *Id2*$^-$ progenitors showed a 2-fold increase in αLP1 and αLP2 after disruption of the Notch pathway (Figures S6A and S6B). Moreover, there was a clear effect of Notch disruption on the αLP2 II subset that decreased from 43% to 26% within the αLP2 compartment. In contrast, αLP2 I was increased (from 17% to 34%), whereas percentages of NKp and LTip (αLP2 III and IV) remained unaffected (Figure 6C).

We further analyzed the expression pattern of αLP2 II to identify which genes are significantly affected by the deletion of Notch signaling in the remaining cells (Figures 6D and 6E). *Hes1* is a well-known target of the Notch signaling. As expected,

(B–E) Gene signatures of different clusters of *Il7r*$^{Cre/+}$*Rbpj*$^{fl/+}$ αLP2, presented as frequency of expression (red = high frequency; blue = low frequency). For (B), genes that were either expressed in the majority or minority of cells and that did not yield in discriminative profile were included.
Data are from two pooled experiments (n = 61 for *Il7r*$^{Cre/+}$*Rbpj*$^{fl/+}$ αLP2, and n = 55 for *Il7r*$^{Cre/+}$*Rbpj*$^{fl/fl}$ αLP2).
See also Figures S3 and S4.

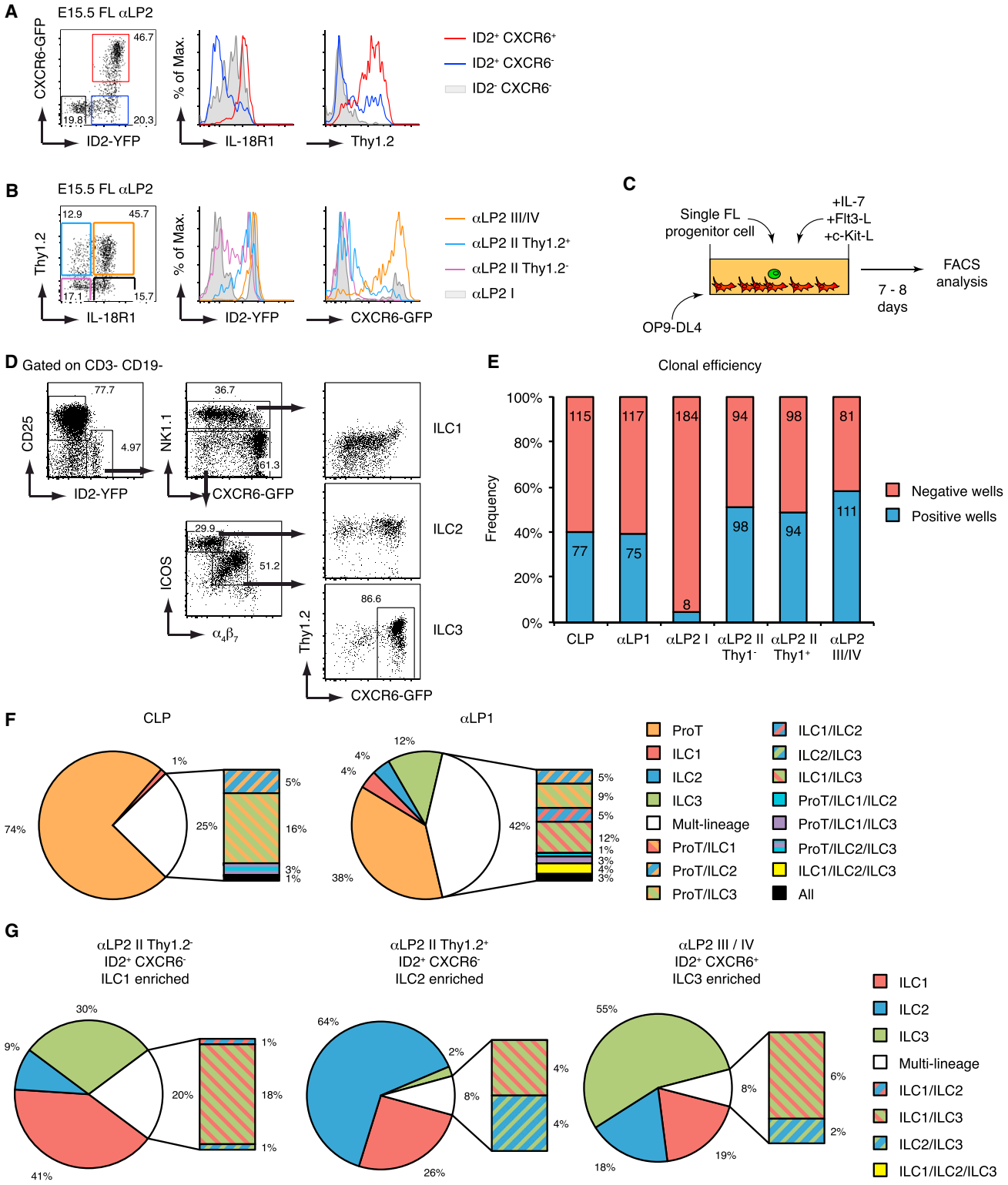

Figure 5. Heterogeneity of αLP2 Subsets Reveals Differential Priming toward ILC Lineages

(A) Flow cytometry of FL cells from *Id2*$^{yfp/+}$*Cxcr6*$^{gfp/+}$ E15.5 embryos. Subdivision of αLP2 according to ID2 and CXCR6 expression, and expression pattern of IL-18R1 and Thy1.2 in ID2^{-}CXCR6^{-} (filled gray), ID2^{+}CXCR6^{-} (blue), or ID2^{+}CXCR6^{+} (red) αLP2.

(B) Subdivision of αLP2 according to IL-18R1 and Thy1.2 expression, and expression pattern of ID2 and CXCR6 in αLP2 I (IL-18R1^{+}Thy1.2^{-}, filled gray), αLP2 II Thy1.2^{-} (IL-18R1^{-}Thy1.2^{-}, violet), αLP2 II Thy1.2^{+} (IL-18R1^{-}Thy1.2^{+}, blue), and αLP2 III/IV (IL-18R1^{+}Thy1.2^{+}, orange).

(legend continued on next page)

the frequency of *Hes1*-expressing cells is reduced from 78% to 47% in the cluster II after disruption of Notch signaling. In the αLP2 compartment, this frequency is decreased from 34% to 12%. Interestingly, *Nfil3* represents the transcription factor most sensitive to the Notch signaling disruption, with a decrease of *Nfil3*$^+$ cells from 74% to 33% of the αLP2 II subset. Milder decreases of gene expression frequencies are also observed for *c-myc*, *Egr1*, and *Cdkn1c*, which are all implicated in cell proliferation; *H19*, which is an oncofetal gene for a non-coding RNA; and *Rora*, which is a key factor of the αLP2 population.

The analysis of the combined expression of key transcription factors (*Rora*, *Gata3*, *Nfil3*, *Hes1*, and *Bcl11b*) uncovers the loss of all cells expressing this set of genes after disruption of the Notch signaling. The few *Tbx21*- or *Rorc*-expressing cells that remain in this subset did not present the same combinatorial diversity as those found in Notch-competent FL (Figure 6E). In conclusion, Notch signaling is active in subset II of the αLP2 compartment.

We analyzed the αLP2 compartments of Notch-competent and -deficient E15.5 FL (Figures 6F and 6G). As expected, no difference was observed in either αLP2 III/IV or αLP2 Thy1.2$^-$ populations after Notch signaling disruption, and the αLP2 I population was increased. In contrast, αLP2 II Thy1.2$^+$ was reduced by one third, confirming that the αLP2 subset is also Notch sensitive ex vivo.

Notch Signaling Acts on the Proliferation, but Not on the Differentiation, of the αLP2 II Thy1.2$^+$ Subset

Finally, we assessed whether Notch signaling could play a role in directing cells toward a given lineage. First, we cultured αLP1 (as control) and αLP2 fractions in short-term cultures with or without Notch inhibitor DAPT and analyzed the progeny, and then we measured their proliferation index (Figures 7A–7C). After 40 hr of culture, proliferation of αLP2 II Thy1.2$^-$ and the αLP2 III/IV subset was not significantly affected. The αLP1 subset gave rise to more ILC precursors in the presence of DAPT, since the development toward the T cell pathway is inhibited (Figure 7C). Only the αLP2 II Thy1.2$^+$ subset was affected by DAPT treatment, resulting in significantly less proliferation (Figure 7C).

We assessed whether Notch disruption would also affect the differentiation potential of each subset of αLP2 by clonal assays as previously described in Figure 5D. As expected, Notch-deficient αLP1 could not give rise to T cells (Figure S7A). αLP2 subsets have similar differentiation potential toward ILC1, ILC2, or ILC3, regardless of Notch signaling (Figure S7B). The differences of output frequencies for αLP2 cultures between WT (*Id2*$^{yfp/+}$ *Cxcr6*$^{gfp/+}$) and *Rbpj* transgenic embryos result from a distinct enrichment in Id2$^+$/CXCR6$^+$ cells among αLP2 fractions (Figure 5B). Indeed, since the αLP2II Thy1.2$^+$ subset still contains few CXCR6$^+$ progenitors in *Rbpj*$^{f/f}$ or *Rbpj*$^{f/+}$, they produce seven times more ILC3 than their WT counterparts devoid of CXCR6$^+$ cells, thanks to the GFP labeling (Figures 5D and S7B). We then compared the clonal efficiencies of αLP1 and αLP2 subsets between Notch-competent and -deficient progenitors. With the exception of the αLP2 II Thy1.2$^+$ subset that was reduced, no difference in the clonal efficiencies was observed for most αLP2 subsets (Figure 7D). Altogether, these results show that the proliferative capacity of the αLP2 II Thy1.2$^+$ compartment is modulated by Notch signaling.

DISCUSSION

By combining clonal in vitro cultures and single-cell gene expression analyses, we determined the pathway of differentiation from the CLP to the different ILC subsets. The combined use of Flt3 and α4β7 already defined CLP, αLP1, and αLP2 (Possot et al., 2011). Here, using ID2/CXCR6 reporter mice, we show that αLP1, while retaining T potential, comprises an all-ILC progenitor at a higher frequency than αLP2, mainly constituted of primed ILC precursors. Supporting this, aLP1 cells express mild levels of ID2. We propose that the GILP is phenotypically defined as Flt3$^+$ ID2^{med}*Tox*$^+$ CXCR6$^-$ in addition to the previous definition of $\alpha_4\beta_7$- and *Nfil3*-expressing cells (Xu et al., 2015). In the single-cell transcriptional analysis, the αLP1 subset encloses *Nfil3*$^+$*Id2*$^-$ cells with a transcriptional profile resembling that of *Nfil3*$^+$*Id2*^{med} cells committed to the ILC lineage. This observation is in accordance with the recent finding that NFIL3 directs the *Id2* expression through IL-7R signaling and control the ILC fate (Xu et al., 2015). However, formal confirmation of the capacity of NFIL3$^+$ cells to be ILC committed before expressing ID2 is still needed. From our single-cell experiment, we can assert that commitment toward the GILP takes place even earlier in the ID2$^+$ fraction of αLP1.

TOX is also an important transcription factor for ILC lineage, since it is found in both αLP1 and αLP2 signatures. TOX-deficient mice lack LTi cells and are devoid of lymph nodes and Peyer's patches, and overexpression of ID2 did not rescue cNK development (Aliahmad et al., 2010). According to a recent report (Seehus et al., 2015), TOX has a role in the early commitment to the ILC fate. Similarly, we show that it is mainly co-expressed with *Nfil3* and *Id2* in αLP1 cells and further maintained in the αLP2 cells.

The transition to the αLP2 stage is accompanied by the decrease of the Flt3 expression and the presence of CXCR6$^+$ cells, which mainly concerns ILC3 primed RORγt$^+$ cells (Possot

(C) Scheme of clonal culture conditions.

(D) Differentiation potential of FL progenitor cells from *Id2*$^{yfp/+}$*Cxcr6*$^{gfp/+}$ E15.5 embryos in conditions depicted in (C). Dot plots represents concatenation of all single wells from an experiment. Readout includes presence of T cell progenitors (CD25$^+$ID2$^-$), ILC1 (ID2$^+$NK1.1$^+$), ILC2 (ID2$^+$NK1.1$^-$ICOS$^{hi}\alpha_4\beta_7^-$), and ILC3 (ID2$^+$NK1.1$^-$ICOS$^{lo}\alpha_4\beta_7^+$CXCR6$^+$).

(E) Clonal efficiency, presented as frequency of positive (blue) and negative (red) wells for hematopoietic cells for each culture subset. Numbers indicate the number of wells that are positive or negative.

(F) Pie chart depicting all possible combinations of readouts after clonal culture of CLP and αLP1 cells. Percentages represent frequency of each combination among positive wells.

(G) Pie chart depicting all possible combinations of readouts after clonal culture of indicated αLP2 subsets. Percentages represent frequency of each combination among positive wells.

Data are representative of at least four independent experiments (A, B, and D) or are from four pooled independent experiments (E–G). In (D)–(G), 192 wells total for each population from four pooled experiments were analyzed.

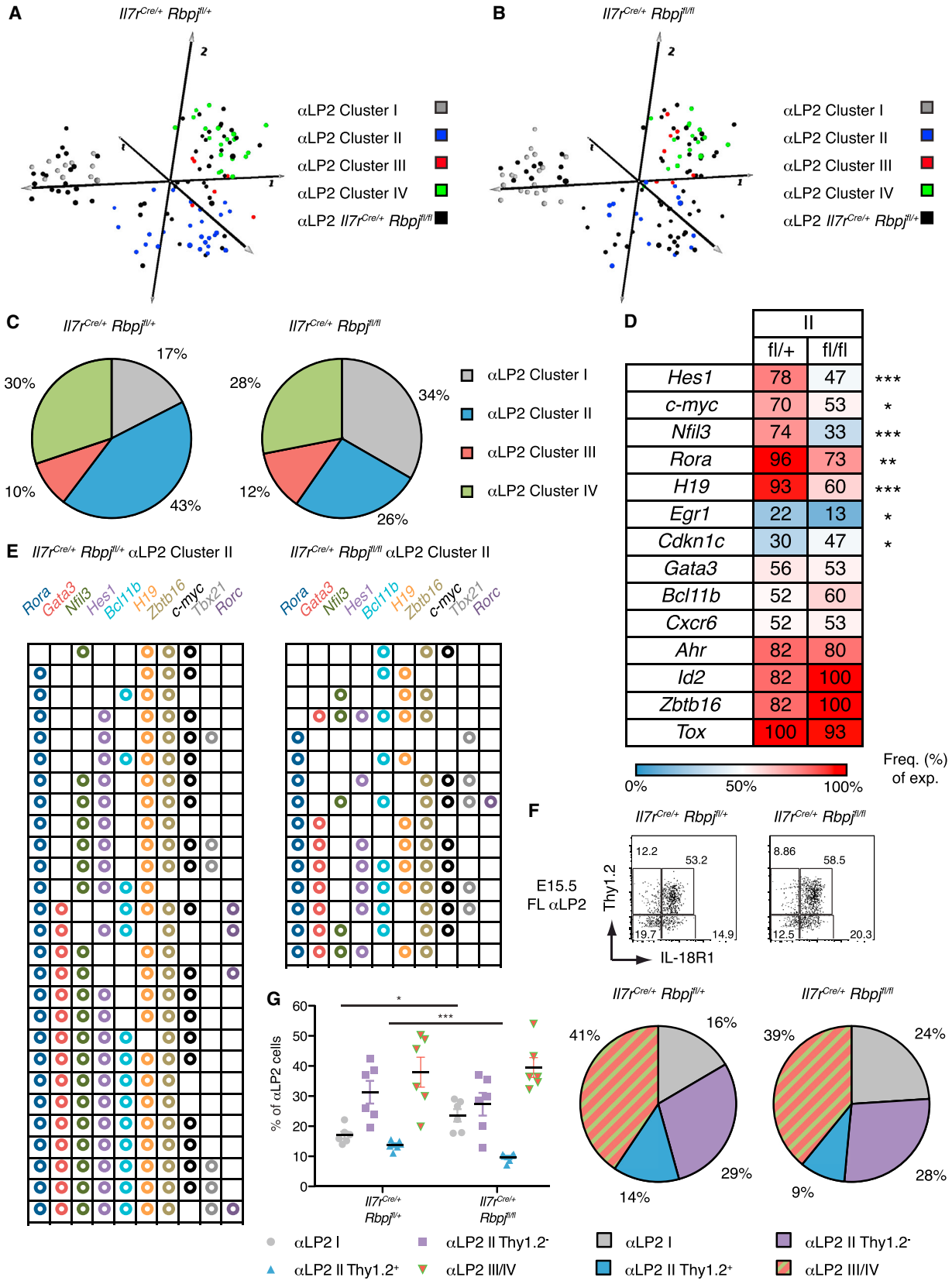

(legend on next page)

et al., 2011). This subset is highly heterogeneous and was separated into four populations thanks to the clustering analysis that displayed diverse enrichment for the expression of the 81 investigated genes. The αLP2 transcriptional signature is defined by the upregulation of ILC-specific markers such as *Notch2*, *Zbtb16*, *Rora*, *Tcf7*, and *Il2rb*. Cluster I contains *Id2*$^-$ progenitors with a quite specific profile different from that of other clusters. Despite the expression of *Nfil3*, these cells were essentially *Tox*$^-$*Tcf7*$^-$*Il2rb*$^-$ and could not differentiate into lymphoid progeny. Thus, we excluded this cluster from the ILC precursor analysis. Using different strategies (clonal cultures and single-cell transcriptomics), we separated subfractions of αLP2 that were already primed for ILC lineages. Transcriptional profiles matched the preferential priming. For example, αLP2 III/IV that is CXCR6$^+$ mainly give rise to ILC3 and, to some extent, ILC1, and it expresses Rorc (in protein and mRNA). It also expresses Tbx21 and Eomes transcripts.

Notch2 levels increase from CLP to αLP2 fraction, inversely to *Notch1* levels. Moreover, *Notch2* expression is maintained in peripheral LTi cells (Possot et al., 2011; Cherrier et al., 2012). Thus, we generated both *Notch2*- and *Rbpj*-deleted embryos in which the Notch pathway was conditionally deleted from the lymphoid progenitor stage, and we calculated that less than 1% of cells escaped the deletion.

CLP, αLP1, αLP2, and LTip fractions from FL were similar in percentage and numbers between Notch-deficient embryos and their control littermates, indicating that Notch signaling is not fundamental for their differentiation. In vitro cultures of Notch-deficient FL CLPs have demonstrated that they upregulate $\alpha_4\beta_7$ within 48 hr independently of Notch signaling. Similarly, the αLP1 and αLP2 precursors from both Notch-competent or -deficient embryos gave rise to identical progenies. A study suggested that Notch signaling must be interrupted after the $\alpha_4\beta_7^+$ stage, since constitutive active Notch signaling results in a block at this precursor stage (Cherrier et al., 2012). When we overexpressed NICD1 in all lymphoid progenitors, we observed accumulation of $\alpha_4\beta_7$ cells that were not *Id2*$^+$ progenitors but *Cd3e*$^+$*Notch1*$^+$ *Dtx1*$^+$ T progenitors. Hence, the absence of LTi cells in mice with a persistent Notch signaling does not result from an arrest at the ILC precursor stage but from an early conversion of lymphoid progenitors into T cell progenitors.

Transcriptional analyses showed that the Notch pathway is then active during ILC differentiation. Notch acts early in ILC development, since the frequency of *Id2*$^+$ progenitors was decreased from the αLP1 stage and to the same extent (more than two times) in the αLP2. This role of the Notch pathway could not be easily detected in vivo, since no marker is available to discern Id2$^+$ from Id2$^-$ cells. Moreover, the *Id2*$^-$ fraction compensated for the loss of *Id2*$^+$ cells in the αLP2 fraction.

ILC and T cells share developmental program similarities. Contrary to T cells, during ILC development, these commonly expressed genes are not significantly decreased after Notch disruption, with the exception of *Hes1*. *Nfil3* is importantly reduced after the Notch pathway disruption, suggesting a possible direct regulation of *Nfil3* by Notch in αLP2 II progenitors. Finally, the abrogation of the Notch pathway changes the distribution of ILC progenitor subsets with a complete loss of *Nfil3*$^+$*Gata3*$^+$*Rora*$^+$*Hes1*$^+$ cells that normally constitute the αLP2 cluster II. We also demonstrated that the Notch pathway is involved in the proliferation of the Thy1.2$^+$ subset of the cluster II, mainly enriched in ILC2 progenitors. Indeed, expression of genes considered as cell-cycle regulators were significantly modified in Notch-deficient embryos. *C-myc* and *Egr1* genes, considered as direct Notch targets in thymocytes, are also significantly decreased in the Thy1.2$^+$ αLP2 subset. These genes have been described as required for the proliferation and survival of thymocytes and downregulated upon inhibition of Notch expression (Dose et al., 2006; Schnell et al., 2006; Sharma et al., 2006). On the contrary, *Cdkn1c*, a negative regulator of cell proliferation and a target of the Notch pathway, is significantly increased in these Notch-deficient Thy1.2$^+$ ILC progenitors (Giovannini et al., 2012). These results are compatible with a study in which progenitors cultured on OP9DL4 gave rise to larger numbers of ILC2 than on OP9 cell lines (Yang et al., 2015).

In conclusion, we show that the Notch pathway is active in both αLP1 and αLP2 compartments, leading to changes in the transcriptional profile, abundance of *Id2*$^+$ progenitors, and proliferation of *Hes1*$^+$ progenitors in Notch-depleted, compared to Notch-competent, embryos. We defined new subsets that are differentially sensitive to the Notch pathway and clarify earlier contradictory in vitro observations. This comparative study indicates that, although it is not essential to the acquisition of $\alpha_4\beta_7$, CXCR6, and RORγt expression by LTip, the Notch pathway is active at different stages along ILC differentiation and in the peripheral pool of LTi cells.

Figure 6. Notch Signaling Disruption Differentially Affects Subsets of αLP2

(A and B) PCA of the single-cell data in Figure 4. Each cluster (identified in Figure 4A) is depicted according to the color key for *Il7r*$^{Cre/+}$*Rbpj*$^{fl/+}$ (A) or *Rbpj*$^{fl/fl}$ (B) αLP2.

(C) Pie charts show percentages of αLP2 I (gray), αLP2 II (blue), αLP2 III (red), or αLP2 IV (green) single cells from *Il7r*$^{Cre/+}$*Rbpj*$^{fl/+}$ (left) or *Rbpj*$^{fl/fl}$ (right) αLP2.

(D) Gene signatures differentially expressed in αLP2 II cells in *Il7r*$^{Cre/+}$*Rbpj*$^{fl/+}$ or *Rbpj*$^{fl/fl}$ FL, presented as frequency of expression (red = high frequency, blue = low frequency).

(E) Combination of expression pattern of selected genes in αLP2 II cells in *Il7r*$^{Cre/+}$*Rbpj*$^{fl/+}$ or *Rbpj*$^{fl/fl}$ FL. Each line represents a single cell, and each column represents the indicated gene.

(F and G) Flow cytometry of E15.5 FL cells from *Il7r*$^{Cre/+}$*Rbpj*$^{fl/+}$ or *Rbpj*$^{fl/fl}$ embryos for the presence of αLP2 subsets, according to IL-18R1 and Thy1.2 expression (F). In (G), percentages of each subset among αLP2 are represented in a dot plot, and pie charts depict the repartition and percentage of each subset in *Il7r*$^{Cre/+}$ *Rbpj*$^{fl/+}$ or *Rbpj*$^{fl/fl}$ αLP2.

Data are from two pooled independent experiments, (A)–(C) (n = 61 for *Il7r*$^{Cre/+}$*Rbpj*$^{fl/+}$ αLP2, and n = 55 for *Il7r*$^{Cre/+}$*Rbpj*$^{fl/fl}$ αLP2) and (D) and (E) (n = 27 for *Il7r*$^{Cre/+}$ *Rbpj*$^{fl/+}$ αLP2 II, and n = 15 for *Il7r*$^{Cre/+}$*Rbpj*$^{fl/fl}$ αLP2 II), are representative of at least four independent experiments (F), or are from four pooled independent experiments (G) (n = 6 single FL from E15.5 *Il7r*$^{Cre/+}$*Rbpj*$^{fl/+}$ or *Rbpj*$^{fl/fl}$ embryos). Statistical data show mean ± SEM. *p < 0.05; **p < 0.01; ***p < 0.001. Unpaired Student's t test was used in (G); chi-square test was used in (D).

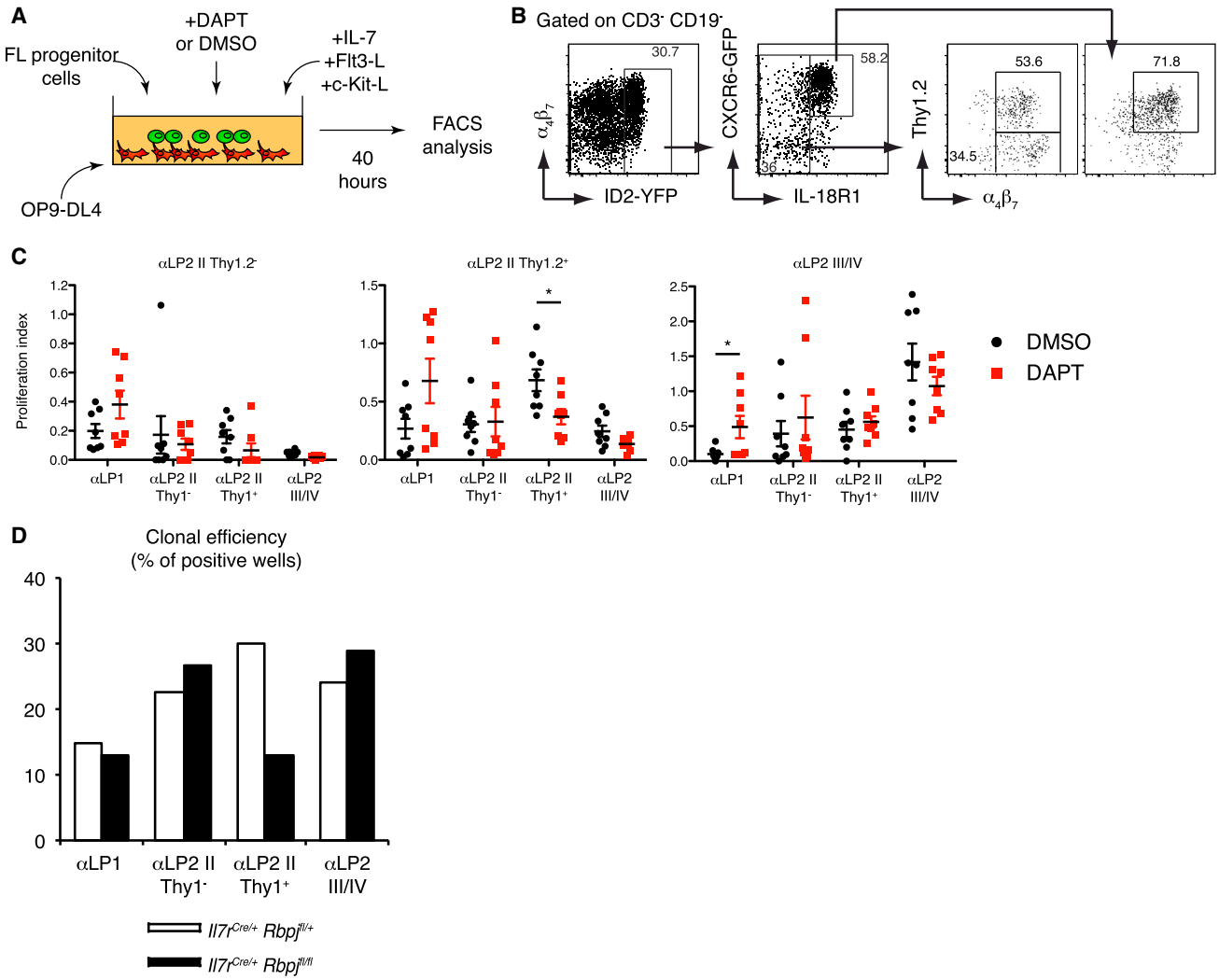

Figure 7. Effect of Notch Signaling on the Proliferation of αLP2 Subsets

(A) Scheme of short-term culture conditions.

(B) Short-term differentiation potential of FL-derived progenitor cells from E15.5 *Id2*$^{YFP/+}$*Cxcr6*$^{GFP/+}$ embryos in conditions depicted in (A). Dot plots represents concatenation of all wells from all populations in culture from an experiment. Cultured cells were analyzed for the presence of αLP2 II Thy1.2^{-}, αLP2 II Thy1.2^{+}, or αLP2 III/IV.

(C) Proliferation index of each subset of the αLP2 population (indicated above each graph) obtained after culture of the indicated αLP cells (indicated on the axis), cultured in the conditions described in (A), in DMSO (black circles) or DAPT (red squares). Proliferation is calculated on the number of cells of each population divided by the number of seeding cells (at least 50 cells in each condition).

(D) Clonal efficiency, presented as frequency of positive wells for each subset from isolated *Il7r*$^{Cre/+}$ *Rbpj*$^{fl/+}$ (white histograms) or *Rbpj*$^{fl/fl}$ E15.5 FL (black histograms). Data are representative of four independent experiments (A–C) or from four pooled independent experiments (D). In (D), each subset was cultured in clonal conditions with the following number of analyzed wells: *Il7r*$^{Cre/+}$*Rbpj*$^{fl/+}$ αLP1 (n = 240), αLP2 II Thy1.2^{-} (n = 240), αLP2 II Thy1.2^{+} (n = 170), αLP2 III/IV (n = 120); and *Il7r*$^{Cre/+}$*Rbpj*$^{fl/+}$ αLP1 (n = 264), αLP2 II Thy1.2^{-} (n = 232), αLP2 II Thy1.2^{+} (n = 137), and αLP2 III/IV (n = 186). In (C), each dot represents a single well from an experiment (two wells per experiment). Statistical data show mean ± SEM. *$p < 0.05$ (unpaired Student's t test).

See also Figure S7.

EXPERIMENTAL PROCEDURES

Mice

Il7r$^{Cre/+}$Rosa26^{YFP} mice (Schlenner et al., 2010) were crossed with Rbpj^{tm1Hon} (Il7r$^{Cre/+}$Rbpj$^{fl/+}$Rosa26^{YFP}), B6.129S-Notch2^{tm3Grid}/J (Il7r$^{Cre/+}$Notch2$^{fl/+}$Rosa26^{YFP}), or Gt(ROSA)26Sor$^{tm(Notch1)Dam}$ (Il7r$^{Cre/+}$Rosa26$^{Nic/+}$).

Id2$^{yfp/+}$*Cxcr6*$^{gfp/+}$ mice were obtained by crossing *Id2*$^{yfp/+}$ *mice* (Yang et al., 2011a) with *Cxcr6*$^{gfp/gfp}$ mice (The Jackson Laboratory). Rorct$^{tg(GFP)}$ mice were provided by G. Eberl. The time of the vaginal plug was considered E0.5. China ink was injected subcutaneously, and lymph nodes were analyzed 2 hr later. All animal experiments were approved by the Pasteur Institute Safety Committee in accordance with the French Ministry of Agriculture and the European Union (EU) guidelines.

Cell Preparation

Fetal organs were harvested, dissociated, and resuspended in Hank's balanced salt solution (HBSS) supplemented with 1% fetal calf serum (FCS) (Gibco). FL cells were depleted of lineage-positive cells by staining with

biotinylated-conjugated antibodies to lineage markers (CD3ε, CD19, CD11c, Ter119, Gr-1, NK1.1), followed by incubation with streptavidin microbeads (Miltenyi Biotec). Depletion was done on LS Columns (Miltenyi Biotec), from which the negative fraction was recovered.

Flow Cytometry and Cell Sorting

Flow cytometry data were acquired using a BD FACSCanto II or BD LSRFortessa (Becton Dickinson) and analyzed with FlowJo software (Tree Star). Dead cells were eliminated by propidium iodide exclusion. Cells were stained intracellularly after permeabilization and fixation with Foxp3 Transcription Factor Fixation/Permeabilization Concentrate and Diluent (eBioscience).

FL, FS, and FmLN cells were purified with a FACSAria III (Becton Dickinson). Cells were recovered in Eppendorf tubes or directly in 96-well qPCR plates for gene expression analysis.

Antibodies

All antibodies were from BD Biosciences, eBioscience, BioLegend, Cell Signaling Technology, or R&D Systems.

Antibodies either biotinylated or conjugated to various fluorochromes were used against the following mouse antigens: Ly76 (TER-119), Gr-1 (RB6-8C5), CD11c (HL3), CD3 (145-2C11), CD19 (6D5), NK1.1 (PK136), IL-7Rα (A7R34), c-Kit (2B8), Sca-1 (D7), RORγt (AFKJS-9), $\alpha_4\beta_7$ (DATK32), Flt3 (A2F10), CD8 (53-6.7), TCRβ (H57-597), CCR6 (29-2L17), CD4 (GK1.5), CD25 (PC61), CD44 (IM7), IL-18R1 (BG/IL18RA), and Thy1.2 (53-2.1).

Cell Culture

All experiments were done in 96-well plates at 37°C and 5% CO_2 and in culture medium consisting of OptiMEM, 10% (v/v) FCS, penicillin (100 U/ml), streptomycin (100 μg/ml) and 2-mercaptoethanol (5×10^{-7} M; GIBCO). OP9 and OP9-DL4 stromal cells were seeded into 96-well plates (1,000 cells per well). The culture medium was supplemented with saturating amounts of c-Kit ligand, Flt3 ligand, IL-2, and IL-7 made "in house." In some experiments, DAPT was added (20 μM, Sigma), with DMSO as control. CLP, αLP1, and αLP2 differentiation potentials were assayed by flow cytometry after 48 hr, 8 days, or 12 days of culture on OP9 or OP9-DL4 stroma.

RT-PCR

Cells were sorted in RLT Buffer (QIAGEN) and were frozen at −80°C. RNA was obtained with an RNeasy Micro Kit (QIAGEN), and cDNA was obtained with a PrimeScript RT Reagent Kit (Takara). A 7300 Real-Time PCR System (Applied Biosystems) and TaqMan technology (Applied Biosystems) or SYBRGreen technology (QIAGEN) were used for RT qPCR. A bilateral unpaired Student's t test was used for statistical analysis.

The following primers were from SABiosciences: *Il17a*, PPM03023A; *Il17f*, PPM05398E; *Il22*, PPM481A; and *Gapdh*, PPM02946E.

The following primers were from Applied Biosystems: *Gata3*, Mm00484683; *Id2*, Mm00711781; *Tox*, Mm00455231_m1; *Hes1*, Mm00468601_m1; *Hprt1*, Mm00446968; *Rbpj*, Mm01217627_g1; *Rora*, Mm01173766_m1; *Rorc*, Mm01261022_m1; *Dtx1*, Mm00492297_m1; *Nrarp*, Mm00482529_s1; *Tcf7*, Mm00493445_m1; *Notch1*, Mm00435249_m1; and *Notch2*, Mm00803069_m1.

The following primers were custom produced by Invitrogen: Cd3e forward: 5′-GCCTCAGAAGCATGATAAGC-3′/ Cd3e reverse: 5′- CCTTGGCCTTCCTATTCTTG-3′.

Biomark

Cells were sorted in 96-well qPCR plates in 10 μl of the CellsDirect One-Step qRT-PCR Kit (Thermo Fisher Scientific), containing a mix of diluted primers (0.05× final concentration; see Tables S1 and S2). Preamplified cDNA was obtained after reverse transcription (15′ at 40°C, 15′ at 50°C and 15′ at 60°C) and preamplification (22 cycles: 15″ at 95°C, 4′ at 60°C) and was diluted 1:5 in TE Buffer[pH 8] (Ambion). Sample mix was as follows: diluted cDNA (2.9 μl), Sample Loading Reagent (0.29 μl, Fluidigm), TaqMan Universal PCR Master Mix (3.3 μl, Applied Biosystems) or Solaris qPCR Low ROX Master Mix (3.3 μl, GE Dharmacon). Assay mix was as follows: Assay Loading Reagent (2.5 μl, Fluidigm), TaqMan (2.5 μl, Applied Biosystems) or Solaris (2.5 μl, GE Dharmacon). A 48.48 or 96.96 dynamic array integrated fluidic circuit (IFC; Fluidigm) was primed with control line fluid, and the chip was loaded with assays (either TaqMan or Solaris) and samples using an HX IFC controller (Fluidigm). The experiments were run on a Biomark HD (Fluidigm) for amplification and detection (2′ at 50°C, 10′ for TaqMan reagents or 15′ for Solaris reagents at 95°C, 40 cycles: 15″ at 95°C, 60″ at 60°C).

Samples that did not express at least one of three housekeeping genes (*Actb*, *Gapdh*, or *Hprt*) were removed from analysis. Data were processed through the MeV (MultiExperiment Viewer) Software (TM4). Hierarchical clustering was performed on C_T values of each gene analyzed from single cells, using uncentered Pearson's correlation with absolute distance and total linkage. PCA was performed to cluster samples.

Statistical Analyses

Statistical data show mean ± SEM. The chi-square test and unpaired Student's t test were used.

SUPPLEMENTAL INFORMATION

Supplemental Information includes seven figures and two tables and can be found with this article online at http://dx.doi.org/10.1016/j.celrep.2016.01.015.

AUTHOR CONTRIBUTIONS

S.C. and S.S. performed most experiments and analyzed data. C.B., T.P., and M.P. performed experiments. O.B.D. performed the mouse genotyping. H.R.R. and A.G. provided mouse lines. A.C. contributed to the writing. R.G. directed research, designed experiments, analyzed data, and wrote the manuscript with input from the coauthors.

ACKNOWLEDGMENTS

We thank A. Bendelac, J.Y. Bertrand, and D. Guy-Grand for critical reading. We are thankful to C. Possot to have started the breeding of the different mouse lines. We acknowledge the Center for Human Immunology and Cytometry platform at Institut Pasteur for support. This work was supported by the Institut Pasteur, INSERM, Université Paris Diderot, and by the Ministère de la Recherche (to S.C.), the Association pour la Recherche sur le Cancer (to S.C. and R.G.), the REVIVE Future Investment Program and the Agence Nationale de Recherche (ANR; grant "Twothyme" to A.C.), the Swiss National Science Foundation and Bourse Roux (to S.S.), ANR grant "Myeloten" (to R.G.), and the Institut National du Cancer (Role of the immune microenvironment during liver carcinogenesis, to R.G.).

Received: August 24, 2015
Revised: December 1, 2015
Accepted: January 2, 2016
Published: January 28, 2016

REFERENCES

Aliahmad, P., de la Torre, B., and Kaye, J. (2010). Shared dependence on the DNA-binding factor TOX for the development of lymphoid tissue-inducer cell and NK cell lineages. Nat. Immunol. *11*, 945–952.

Bernink, J.H., Peters, C.P., Munneke, M., te Velde, A.A., Meijer, S.L., Weijer, K., Hreggvidsdottir, H.S., Heinsbroek, S.E., Legrand, N., Buskens, C.J., et al. (2013). Human type 1 innate lymphoid cells accumulate in inflamed mucosal tissues. Nat. Immunol. *14*, 221–229.

Cherrier, M., Sawa, S., and Eberl, G. (2012). Notch, Id2, and RORγt sequentially orchestrate the fetal development of lymphoid tissue inducer cells. J. Exp. Med. *209*, 729–740.

Constantinides, M.G., McDonald, B.D., Verhoef, P.A., and Bendelac, A. (2014). A committed precursor to innate lymphoid cells. Nature *508*, 397–401.

Daussy, C., Faure, F., Mayol, K., Viel, S., Gasteiger, G., Charrier, E., Bienvenu, J., Henry, T., Debien, E., Hasan, U.A., et al. (2014). T-bet and Eomes instruct the development of two distinct natural killer cell lineages in the liver and in the bone marrow. J. Exp. Med. *211*, 563–577.

Dose, M., Khan, I., Guo, Z., Kovalovsky, D., Krueger, A., von Boehmer, H., Khazaie, K., and Gounari, F. (2006). c-Myc mediates pre-TCR-induced proliferation but not developmental progression. Blood *108*, 2669–2677.

Eberl, G., Marmon, S., Sunshine, M.J., Rennert, P.D., Choi, Y., and Littman, D.R. (2004). An essential function for the nuclear receptor RORgamma(t) in the generation of fetal lymphoid tissue inducer cells. Nat. Immunol. *5*, 64–73.

Fuchs, A., Vermi, W., Lee, J.S., Lonardi, S., Gilfillan, S., Newberry, R.D., Cella, M., and Colonna, M. (2013). Intraepithelial type 1 innate lymphoid cells are a unique subset of IL-12- and IL-15-responsive IFN-γ-producing cells. Immunity *38*, 769–781.

Giovannini, C., Gramantieri, L., Minguzzi, M., Fornari, F., Chieco, P., Grazi, G.L., and Bolondi, L. (2012). CDKN1C/P57 is regulated by the Notch target gene Hes1 and induces senescence in human hepatocellular carcinoma. Am. J. Pathol. *181*, 413–422.

Han, H., Tanigaki, K., Yamamoto, N., Kuroda, K., Yoshimoto, M., Nakahata, T., Ikuta, K., and Honjo, T. (2002). Inducible gene knockout of transcription factor recombination signal binding protein-J reveals its essential role in T versus B lineage decision. Int. Immunol. *14*, 637–645.

Hori, K., Sen, A., and Artavanis-Tsakonas, S. (2013). Notch signaling at a glance. J. Cell Sci. *126*, 2135–2140.

Hoyler, T., Klose, C.S., Souabni, A., Turqueti-Neves, A., Pfeifer, D., Rawlins, E.L., Voehringer, D., Busslinger, M., and Diefenbach, A. (2012). The transcription factor GATA-3 controls cell fate and maintenance of type 2 innate lymphoid cells. Immunity *37*, 634–648.

Iso, T., Kedes, L., and Hamamori, Y. (2003). HES and HERP families: multiple effectors of the Notch signaling pathway. J. Cell. Physiol. *194*, 237–255.

Klein Wolterink, R.G., Serafini, N., van Nimwegen, M., Vosshenrich, C.A., de Bruijn, M.J., Fonseca Pereira, D., Veiga Fernandes, H., Hendriks, R.W., and Di Santo, J.P. (2013). Essential, dose-dependent role for the transcription factor Gata3 in the development of IL-5+ and IL-13+ type 2 innate lymphoid cells. Proc. Natl. Acad. Sci. USA *110*, 10240–10245.

Klose, C.S., Kiss, E.A., Schwierzeck, V., Ebert, K., Hoyler, T., d'Hargues, Y., Göppert, N., Croxford, A.L., Waisman, A., Tanriver, Y., and Diefenbach, A. (2013). A T-bet gradient controls the fate and function of CCR6-RORγt+ innate lymphoid cells. Nature *494*, 261–265.

Klose, C.S., Flach, M., Möhle, L., Rogell, L., Hoyler, T., Ebert, K., Fabiunke, C., Pfeifer, D., Sexl, V., Fonseca-Pereira, D., et al. (2014). Differentiation of type 1 ILCs from a common progenitor to all helper-like innate lymphoid cell lineages. Cell *157*, 340–356.

Kondo, M., Weissman, I.L., and Akashi, K. (1997). Identification of clonogenic common lymphoid progenitors in mouse bone marrow. Cell *91*, 661–672.

Lee, J.S., Cella, M., McDonald, K.G., Garlanda, C., Kennedy, G.D., Nukaya, M., Mantovani, A., Kopan, R., Bradfield, C.A., Newberry, R.D., and Colonna, M. (2012). AHR drives the development of gut ILC22 cells and postnatal lymphoid tissues via pathways dependent on and independent of Notch. Nat. Immunol. *13*, 144–151.

Lewis, K.L., Caton, M.L., Bogunovic, M., Greter, M., Grajkowska, L.T., Ng, D., Klinakis, A., Charo, I.F., Jung, S., Gommerman, J.L., et al. (2011). Notch2 receptor signaling controls functional differentiation of dendritic cells in the spleen and intestine. Immunity *35*, 780–791.

Mebius, R.E., Miyamoto, T., Christensen, J., Domen, J., Cupedo, T., Weissman, I.L., and Akashi, K. (2001). The fetal liver counterpart of adult common lymphoid progenitors gives rise to all lymphoid lineages, CD45+CD4+CD3- cells, as well as macrophages. J. Immunol. *166*, 6593–6601.

Moro, K., Yamada, T., Tanabe, M., Takeuchi, T., Ikawa, T., Kawamoto, H., Furusawa, J., Ohtani, M., Fujii, H., and Koyasu, S. (2010). Innate production of T(H)2 cytokines by adipose tissue-associated c-Kit(+)Sca-1(+) lymphoid cells. Nature *463*, 540–544.

Oh, P., Lobry, C., Gao, J., Tikhonova, A., Loizou, E., Manent, J., van Handel, B., Ibrahim, S., Greve, J., Mikkola, H., et al. (2013). In vivo mapping of notch pathway activity in normal and stress hematopoiesis. Cell Stem Cell *13*, 190–204.

Possot, C., Schmutz, S., Chea, S., Boucontet, L., Louise, A., Cumano, A., and Golub, R. (2011). Notch signaling is necessary for adult, but not fetal, development of RORγt(+) innate lymphoid cells. Nat. Immunol. *12*, 949–958.

Pui, J.C., Allman, D., Xu, L., DeRocco, S., Karnell, F.G., Bakkour, S., Lee, J.Y., Kadesch, T., Hardy, R.R., Aster, J.C., and Pear, W.S. (1999). Notch1 expression in early lymphopoiesis influences B versus T lineage determination. Immunity *11*, 299–308.

Rankin, L.C., Groom, J.R., Chopin, M., Herold, M.J., Walker, J.A., Mielke, L.A., McKenzie, A.N., Carotta, S., Nutt, S.L., and Belz, G.T. (2013). The transcription factor T-bet is essential for the development of NKp46+ innate lymphocytes via the Notch pathway. Nat. Immunol. *14*, 389–395.

Saito, T., Chiba, S., Ichikawa, M., Kunisato, A., Asai, T., Shimizu, K., Yamaguchi, T., Yamamoto, G., Seo, S., Kumano, K., et al. (2003). Notch2 is preferentially expressed in mature B cells and indispensable for marginal zone B lineage development. Immunity *18*, 675–685.

Sambandam, A., Maillard, I., Zediak, V.P., Xu, L., Gerstein, R.M., Aster, J.C., Pear, W.S., and Bhandoola, A. (2005). Notch signaling controls the generation and differentiation of early T lineage progenitors. Nat. Immunol. *6*, 663–670.

Satoh-Takayama, N., Lesjean-Pottier, S., Vieira, P., Sawa, S., Eberl, G., Vosshenrich, C.A., and Di Santo, J.P. (2010). IL-7 and IL-15 independently program the differentiation of intestinal CD3-NKp46+ cell subsets from Id2-dependent precursors. J. Exp. Med. *207*, 273–280.

Satpathy, A.T., Briseño, C.G., Lee, J.S., Ng, D., Manieri, N.A., Kc, W., Wu, X., Thomas, S.R., Lee, W.L., Turkoz, M., et al. (2013). Notch2-dependent classical dendritic cells orchestrate intestinal immunity to attaching-and-effacing bacterial pathogens. Nat. Immunol. *14*, 937–948.

Sawa, S., Cherrier, M., Lochner, M., Satoh-Takayama, N., Fehling, H.J., Langa, F., Di Santo, J.P., and Eberl, G. (2010). Lineage relationship analysis of RORgammat+ innate lymphoid cells. Science *330*, 665–669.

Schlenner, S.M., Madan, V., Busch, K., Tietz, A., Läufle, C., Costa, C., Blum, C., Fehling, H.J., and Rodewald, H.R. (2010). Fate mapping reveals separate origins of T cells and myeloid lineages in the thymus. Immunity *32*, 426–436.

Schmutz, S., Bosco, N., Chappaz, S., Boyman, O., Acha-Orbea, H., Ceredig, R., Rolink, A.G., and Finke, D. (2009). Cutting edge: IL-7 regulates the peripheral pool of adult ROR gamma+ lymphoid tissue inducer cells. J. Immunol. *183*, 2217–2221.

Schnell, F.J., Zoller, A.L., Patel, S.R., Williams, I.R., and Kersh, G.J. (2006). Early growth response gene 1 provides negative feedback to inhibit entry of progenitor cells into the thymus. J. Immunol. *176*, 4740–4747.

Seehus, C.R., Aliahmad, P., de la Torre, B., Iliev, I.D., Spurka, L., Funari, V.A., and Kaye, J. (2015). The development of innate lymphoid cells requires TOX-dependent generation of a common innate lymphoid cell progenitor. Nat. Immunol. *16*, 599–608.

Seillet, C., Belz, G.T., and Mielke, L.A. (2014). Complexity of cytokine network regulation of innate lymphoid cells in protective immunity. Cytokine *70*, 1–10.

Serafini, N., Klein Wolterink, R.G., Satoh-Takayama, N., Xu, W., Vosshenrich, C.A., Hendriks, R.W., and Di Santo, J.P. (2014). Gata3 drives development of RORγt+ group 3 innate lymphoid cells. J. Exp. Med. *211*, 199–208.

Sharma, V.M., Calvo, J.A., Draheim, K.M., Cunningham, L.A., Hermance, N., Beverly, L., Krishnamoorthy, V., Bhasin, M., Capobianco, A.J., and Kelliher, M.A. (2006). Notch1 contributes to mouse T-cell leukemia by directly inducing the expression of c-myc. Mol. Cell. Biol. *26*, 8022–8031.

Tanigaki, K., Han, H., Yamamoto, N., Tashiro, K., Ikegawa, M., Kuroda, K., Suzuki, A., Nakano, T., and Honjo, T. (2002). Notch-RBP-J signaling is involved in cell fate determination of marginal zone B cells. Nat. Immunol. *3*, 443–450.

Wong, S.H., Walker, J.A., Jolin, H.E., Drynan, L.F., Hams, E., Camelo, A., Barlow, J.L., Neill, D.R., Panova, V., Koch, U., et al. (2012). Transcription factor RORα is critical for nuocyte development. Nat. Immunol. *13*, 229–236.

Xu, W., Domingues, R.G., Fonseca-Pereira, D., Ferreira, M., Ribeiro, H., Lopez-Lastra, S., Motomura, Y., Moreira-Santos, L., Bihl, F., Braud, V., et al. (2015). NFIL3 orchestrates the emergence of common helper innate lymphoid cell precursors. Cell Rep. *10*, 2043–2054.

Yang, C.Y., Best, J.A., Knell, J., Yang, E., Sheridan, A.D., Jesionek, A.K., Li, H.S., Rivera, R.R., Lind, K.C., D'Cruz, L.M., et al. (2011a). The transcriptional regulators Id2 and Id3 control the formation of distinct memory CD8+ T cell subsets. Nat. Immunol. *12*, 1221–1229.

Yang, Q., Saenz, S.A., Zlotoff, D.A., Artis, D., and Bhandoola, A. (2011b). Cutting edge: Natural helper cells derive from lymphoid progenitors. J. Immunol. *187*, 5505–5509.

Yang, Q., Li, F., Harly, C., Xing, S., Ye, L., Xia, X., Wang, H., Wang, X., Yu, S., Zhou, X., et al. (2015). TCF-1 upregulation identifies early innate lymphoid progenitors in the bone marrow. Nat. Immunol. *16*, 1044–1050.

Yokota, Y., Mansouri, A., Mori, S., Sugawara, S., Adachi, S., Nishikawa, S., and Gruss, P. (1999). Development of peripheral lymphoid organs and natural killer cells depends on the helix-loop-helix inhibitor Id2. Nature *397*, 702–706.

Yoshida, H., Naito, A., Inoue, J., Satoh, M., Santee-Cooper, S.M., Ware, C.F., Togawa, A., Nishikawa, S., and Nishikawa, S. (2002). Different cytokines induce surface lymphotoxin-alphabeta on IL-7 receptor-alpha cells that differentially engender lymph nodes and Peyer's patches. Immunity *17*, 823–833.